

# DOE-FIU SCIENCE & TECHNOLOGY WORKFORCE DEVELOPMENT PROGRAM

## STUDENT SUMMER INTERNSHIP TECHNICAL REPORT

June 2, 2010 to August 7, 2010

# Uranium Toxicity to Native Microbial Communities in the Hanford 300 Area Groundwater

### Principal Investigators:

Denny A. Carvajal (DOE Fellow)  
Florida International University

Andrew E. Plymale, Mentor  
Pacific Northwest National Laboratory

Dr. Allan Konopka, Mentor  
Pacific Northwest National Laboratory

Dr. Jim Friedrichson, Mentor  
Pacific Northwest National Laboratory

### Acknowledgements:

Dr. Xueju Lin, Dr. Ji-Hoon Li, Dr. James P. McKinley  
Pacific Northwest National Laboratory

### Florida International University Collaborator:

Yelena Katsenovich, Ph.D

### Florida International University Collaborator and Program Director:

Leonel Lagos, Ph.D., PMP®

### Prepared for:

U.S. Department of Energy  
Office of Environmental Management  
Under Grant No. DE-FG01-05EW07033

### **DISCLAIMER**

This report was prepared as an account of work sponsored by an agency of the United States government. Neither the United States government nor any agency thereof, nor any of their employees, nor any of its contractors, subcontractors, nor their employees makes any warranty, express or implied, or assumes any legal liability or responsibility for the accuracy, completeness, or usefulness of any information, apparatus, product, or process disclosed, or represents that its use would not infringe upon privately owned rights. Reference herein to any specific commercial product, process, or service by trade name, trademark, manufacturer, or otherwise does not necessarily constitute or imply its endorsement, recommendation, or favoring by the United States government or any other agency thereof. The views and opinions of authors expressed herein do not necessarily state or reflect those of the United States government or any agency thereof.

## ABSTRACT

---

This study was undertaken to better understand the mobility of uranium due to reduction and sorption and the toxic effects of uranium on native microbial cultures found in the uranium contaminated soil and groundwater of the Hanford 300 Area, near the Columbia River in southeastern Washington state. Different factors can affect the reduction and sorption kinetic rates and bioavailability of free and complexed uranium (i.e. hydroxyl and carbonate complexes) in the environment. These factors include uranium concentration, pH, bicarbonate concentrations, cell density, and calcium concentrations, which could be significant in determining whether microbes play an important role on the biogeochemistry of uranium. For example, uranium could be mobilized back into the environment or reduced and sequestered by the microbes. In this report, we determine the toxic concentrations of uranium to the native microbial populations in different aqueous environments (carbonate-free synthetic groundwater and carbonate-containing groundwater) and determine whether the microbes are resilient enough to withstand high concentration levels of uranium. The <sup>3</sup>H-Leucine incorporation method was implemented to quantify the microbial biomass activity. Results show that carbonate is a dominant variable that determines the uranium speciation and toxicity to the microbial community. It is probable that natural groundwater carbonate concentrations safeguard the microbial population by increasing its lethal dose (LD<sub>50</sub>) from 0.3 uM to ≈500 uM of uranium when only approximately 0.25 mM HCO<sub>3</sub> from atmospheric CO<sub>2</sub> is present. Cell density differences did not show different toxic effects due to uranium concentrations ranging from 0-5 uM without added carbonate. The research presented here is part of a large effort to advance the understanding of the biogeochemistry processes and plausible remediation strategies concerning the uranium plume in the Hanford 300 Area.

## TABLE OF CONTENTS

---

ABSTRACT.....	iii
TABLE OF CONTENTS.....	iv
LIST OF FIGURES .....	v
LIST OF TABLES.....	vii
EXECUTIVE SUMMARY .....	1
1. BACKGROUND .....	2
2. THEORY .....	7
2.1 Uranium .....	7
2.2 Microbial Adsorption Proof.....	9
2.3 Uranium Sorption & Toxicity Mechanism .....	10
2.4 Effects of pH.....	12
2.5 Effects of Phosphate .....	13
2.6 Effects of Carbonate .....	14
2.7 Effects of Calcium .....	14
3. RESEARCH DESCRIPTIONS .....	16
3.1 Cell Preparation .....	16
3.2 Synthetic Groundwater .....	16
3.3 Nutrient Limiting Factor .....	19
3.4 Uptake Kinetics & Biosorption.....	19
3.5 Test Chamber/ Bioreactor .....	21
3.6 Modeling.....	21
3.7 Measuring Bacterial Biomass Production and Growth Rates from Leucine Incorporation in Natural Aquatic Environments .....	24
3.8 Protocol: Measuring 3H-Leucine Incorporation by the Microcentrifuge Method (Kirchman).....	27
3.9 Cell Count Microscopy .....	27
4. RESULTS AND DISCUSSION .....	29
4.1 3H-Leucine Uptake Kinetics .....	29
5. CONCLUSION.....	39
6. FUTURE WORK.....	40
7. REFERENCES .....	41

## LIST OF FIGURES

---

Figure 1. [Left] Aerial photograph of the 300 Area north process pond (NNP) in 2003, after excavation of the residual pond wastes (Source: McKinley). [Right] Aerial photograph of the 300 Area site (Source: Xueju Lin).	3
Figure 2. Uranium plume concentrations in the Hanford Site, 300 Area (Source: McKinley). The excavated process ponds were located near the river shore. The process ponds (PP) sample locations are indicated.	3
Figure 3. Summary of uranium and tracer response data at the Integrated Field Research Challenge (IFRC) Well Field in the south process pond	4
Figure 4. Relative abundance of microbial populations found in the Hanford 300 Area with respect to depth (Source: Xueju Lin).	5
Figure 5. Typical UV-VIS spectra of the A) control, B) citrate, C) NTA, and D) EDTA media at 0, 2, 4, 8, 21, 28, and 50 hours after inoculation with <i>S. putrefaciens</i> .	8
Figure 6. Schematic illustration of a variety of molecular environmental science processes affecting contaminant elements in soils and ground water (Source: Gordon E. Brown).	11
Figure 7. Uranium detoxification model in <i>Desulfovibrio desulfuricans</i> G20. NAD(P)H = reduced form of nicotinamide adenine dinucleotide phosphate; U(VI) = reduced uranium: U(IV) = uranium (VI) (Source: Sani).	12
Figure 8. Effect of pH on removal of soluble uranium u(VI) by granular biomass. A) U(VI) uptake at different initial pH values determined after 1 h contact time. B) Time course of u(VI) biosorption at pH 4 and pH 7 (initial (UVI) concentration: 100 mg/L, error bars : $\pm 1$ SD. (Source: Nancharaiah)	13
Figure 9. Survival of the culturable population with time, including the die-off portion of the population. Typical direct count enumeration data are also shown. The difference between direct and culturable counts represents the population that remained viable but not culturable by routine or standard microbiological methods (Source: Roszak).	16
Figure 10. Time-dependence of uranium uptake at a total concentration of 200nM (Black dots->intracellular; white dots->Extracellular). Error bars n=3. (Source: Fortin).	21
Figure 11. Biosorption of uranium from solutions of different initial uranium concentrations. Specific uptake of uranium ( $\text{mg U g}^{-1}$ dry biomass) was plotted as a function of uranium remaining in the solution after 24h incubation time. (Source: Nancharaiah)	22
Figure 12. Example of bacterial biomass exponential growth.	25
Figure 13. Leucine amino acid.	25
Figure 14. [Left] Groundwater collected 5-10-10. Well 2-21 (water table depth- 31 ft bgs) was bailed, while well 2-27 (deep) was pumped. Leucine was at 500 nM (2.5 uCi/sample). Incubation was at RT (static). [Right] Groundwater from wells 2-26 & 2-27 with 500 nM 3H leucine in 10 hr incubation time with 0.25X, 0.5X, and 1X the natural cell density. Provided by Andrew E. Plymale.	29

Figure 15. Groundwater was collected 5-29-10. Both well 2-26 (water table depth) and well 2-27 (deep) were pumped. Leucine was at 500 nM (2.5 uCi/sample). Samples were incubated with 3H-Leu for 10 h (RT, static). All treatments contained 2.5 mM added NaHCO <sub>3</sub> and were diluted 9/10 in the NaHCO <sub>3</sub> /U(VI) stock. Provided by Andrew E. Plymale. (n=3) .....	30
Figure 16. 3H-Leucine incorporated uranium toxicity study: 300A GW bacteria from the deep & shallow wells in CO <sub>3</sub> -Free PIPES SGW Vs high uranium concentrations (pH 6.7). All treatments killed more than 50% of the microbial population, thus all treatments were above the lethal dose of uranium under these conditions. (n=3) .....	31
Figure 17. 3H-Leucine incorporated uranium toxicity study: 300A GW bacteria resuspended in CO <sub>3</sub> -free HEPES SGW pH 7.7 (2 mM HEPES, ~ 0.25 mM HCO <sub>3</sub> <sup>-</sup> from atmospheric CO <sub>2</sub> ) vs Low uranium concentrations from: A) the deep wells, B) shallow wells. Lethal dose occurs at the 0.3 uM of Uranium. (n=3) .....	32
Figure 18. Cell density (cells/ml) of microbes fresh from the groundwater vs. cell density (cells/ml) of microbes filtered and re-suspended in the synthetic groundwater used for experiments from both the deep (2-27) and shallow (2-26) wells. ....	33
Figure 19. Fluorescent microscopy camera field view of the Cybergreen Fluorescence staining on the 2-27 (deep) & 2-26 (shallow) 300 Area microbes (left and right respectively). (Source: Dr. Xueju Lin).....	33
Figure 20. 3H-Leucine incorporated uranium toxicity study: 300A GW bacteria resuspended in CO <sub>3</sub> -free HEPES SGW pH 7.7 (2 mM HEPES, ~ 0.25 mM HCO <sub>3</sub> <sup>-</sup> from atmospheric CO <sub>2</sub> ) vs Low uranium concentrations from: Top) 2-26 shallow well. Bottom) 3-23 shallow well. (n=3) ..	34
Figure 21. Cell density (cells/ml) of microbes filtered and re-suspended in the synthetic groundwater used for experiments from both the (3-23) and (2-26) shallow wells. ....	35
Figure 22. Fluorescent microscopy camera field view of the Cybergreen Fluorescence staining on the 300 Area microbes of the 3-23 & 2-26 wells (left and right respectively). (Source: Dr. Xueju Lin).....	35
Figure 23. Measured natural uranium background concentrations over time for the 300 Area groundwater via KPA analysis.....	36
Figure 24. Relative inhibition vs. U(VI) concentration in CO free SGW, (top) 7/7/10 experiments, (bottom) 7/27/10 experiments. Toxic power (n) model. ....	36
Figure 25. U toxicity to bacteria as 3H-Leu % uptake from 300A groundwater re-suspended in CO <sub>3</sub> -free SGW, pH 7.7 (2 mM HEPES, ~ 0.25 mM HCO <sub>3</sub> <sup>-</sup> from atmospheric CO <sub>2</sub> ), and concentration of uranium positive species vs uranium concentration. ....	37
Figure 27. 3H-Leucine uptake by bacteria desorbed from Hanford (left) and Ringold (right) sediments amended with C, N, and P. Produced and provided by Andrew E. Plymale.....	38
Figure 26. MINTEQA2 uranium speciation modeling: [Species] vs. increasing [HCO <sub>3</sub> ] added to SGW with 0.31 uM (U(VI)) with atmospheric equilibration (~0.2 mM HCO <sub>3</sub> ). ....	38

## LIST OF TABLES

---

Table 1. Groundwater Composition and Uranium Speciation.....	17
Table 2. Comparison of SPPP1 Natural and Synthetic Groundwater.....	18
Table 3. Specific Salt Additions to Produce 1L of Synthetic Groundwater (SGW-SPP1).....	18
Table 4. Stock Solutions for SGW-SPPP1 .....	19
Table 5. Carbonate Free Synthetic Groundwater.....	19
Table 6. Parameters used in Modeling Tracers and U(VI) Adsorption/Desorption for ICE I.....	23

## EXECUTIVE SUMMARY

---

This research work has been supported by the DOE-FIU Science & Technology Workforce Initiative, an innovative program developed by the US Department of Energy's Environmental Management (DOE-EM) and Florida International University's Applied Research Center (FIU-ARC). During the summer of 2010, a DOE Fellow intern (Mr. Denny Carvajal) spent 10 weeks doing a summer internship at the Pacific Northwest National Laboratory (PNNL) in the Microbiology group under the supervision and guidance of Mr. A. E. Plymale, Dr. J. Friedrichson, and Dr. A. Konopka. This internship was coordinated with the PNNL Office of Science and Engineering Education (SEE) and fell under the category of Alternate Sponsored Fellow (ASF). The DOE Fellow's project was initiated on June 2, 2010, and continued through August 7, 2010, with the objectives of 1) acquiring new skills and knowledge relevant to a similar assignment as FIU's Applied Research Center (ARC) project #2, "Rapid Deployment of Engineered Solutions for Environmental Problems at Hanford," which could result in future collaborative work, and 2) making contributions toward a master's thesis based on the experimental work performed during the internship. During this internship, the student received extensive radiological training before conducting experiments with radiological materials. The purpose of the laboratory work conducted during this internship was to study the toxic effects of different concentration of uranium species on the native microbes in the Hanford 300-Area groundwater; these results will aid in the understanding of the ongoing biogeochemical processes in the transport and sequestration of uranium at the Hanford site 300-Area which may have potential as a bioremediation strategy.

## 1. BACKGROUND

---

From 1943 until 1989, the Hanford Site in Washington State produced plutonium for weapons applications. The Hanford Site occupies approximately 1,500 km<sup>2</sup> in an arid environment, bounded by the Columbia River to the east and by the Rattlesnake Mountain to the west. Fuel fabrication occurred at the site's southern extremity (300 Area); fuel was irradiated near the Columbia River to the north (100 Areas); and the rods were processed in chemical facilities on the site's central plateau (200 Area). Each of the manufacturing components had a characteristic waste stream or streams, and while some streams were disposed directly onto the ground surface, other streams were retained for long-term storage or isolation. Materials research and fabrication at the 300 Area generated wastes that were sluiced into process ponds (Figure 1), constructed and maintained to avoid contamination of the nearby Columbia River less than 1000 feet away. The ponds received constant and intermittent releases of waste of a broad variety in composition and volume, including caustic alkaline and acidic fluids and slurries containing uranium, aluminum, and copper. The North and South 300 Area Process Ponds (in the 300-FF-5 Operable Unit) received long-term seepage/spills of acidic or neutral uranium wastes (58,000 kg of disposed uranium over 32 yr) to the thin and shallow 300 Area vadose zone (Hanford formation sediment, primarily flood deposited sands and gravels). Released uranium into the same surficial sedimentary deposit represents a source or potential source of uranium to groundwater. Similarly, at the 200 East Area BX tank farm, 7,000 kg of uranium were spilled in one event. The pH of the pond water was temporally variable, ranging from 1.8 to 11.4. Sodium hydroxide was frequently added when the pH was acidic to minimize leaching of copper (Cu) and uranium (U) through the vadose zone into the underlying unconfined aquifer and into the Columbia River. However, waste disposal resulted in a groundwater plume of U(VI) (Figure 2) that persists today. As part of the Environmental Remediation Sciences Program (ERSP), and from the Hanford Integrated Field Research Challenge (IFRC) at Pacific Northwest National Laboratory, James P. McKinley has determined that the Columbia River exhibits large seasonal discharge/stage variations, particularly in the spring, which propagate directly into the near-river groundwater aquifer in the form of water table fluctuations. A persistent U plume exists in the aquifer, hypothesized to originate from U captured by the rising water table, over the extent of its annual vertical excursion (the 'smear zone'). Due to these water table fluctuations, multiple rise-and-fall cycles in the river, uranium monitored levels in some wells varied greatly from ~50 ug/L to >300ug/L (McKinley 2007). The 300 Area sediments included metatorbernite  $\text{Cu}(\text{UO}_2)_2(\text{PO}_4)_2 \cdot 8(\text{H}_2\text{O})$  and uranium at low concentrations associated with detrital aluminosilicates, along with other mineral phases that could accommodate uranyl, such as uranophane and calcium carbonate. The association of contaminant uranyl with Hanford formation sediments provides a persistent source of uranium to groundwater (McKinley 2007). Physico-chemical remediation methods for radioactive contaminants with long-term environmental risks like uranium are a problem since they are usually expensive and not always a suitable cost-effective response (Nancharaiyah). A sound and reasonable alternative is exploiting native microbes in the soil to remove highly soluble contaminants such as uranium, by reducing it from U(VI) to U(IV) as insoluble uraninite, from the groundwater if they are capable and efficient (Kelly 2005). However, little is known about the role of microbes and their biogeochemistry processes involving uranium in the field. As a result of the expense and

difficulty of remediation efforts for uranium, numerous basic and applied studies of uranium mobility have been undertaken in the USA and elsewhere; here the focus is on improving the understanding of the role the microbiological community native to the 300 Area has on the persistent uranium plume.

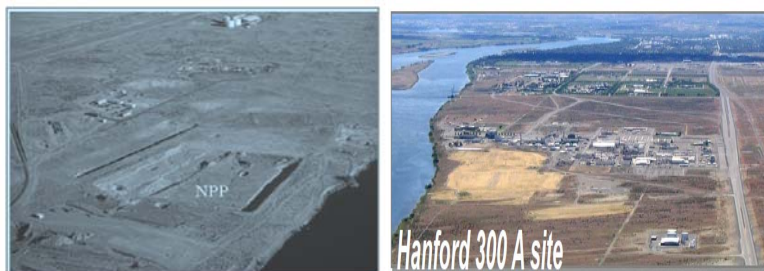


Figure 1. [Left] Aerial photograph of the 300 Area north process pond (NPP) in 2003, after excavation of the residual pond wastes (Source: McKinley). [Right] Aerial photograph of the 300 Area site (Source: Xueju Lin).

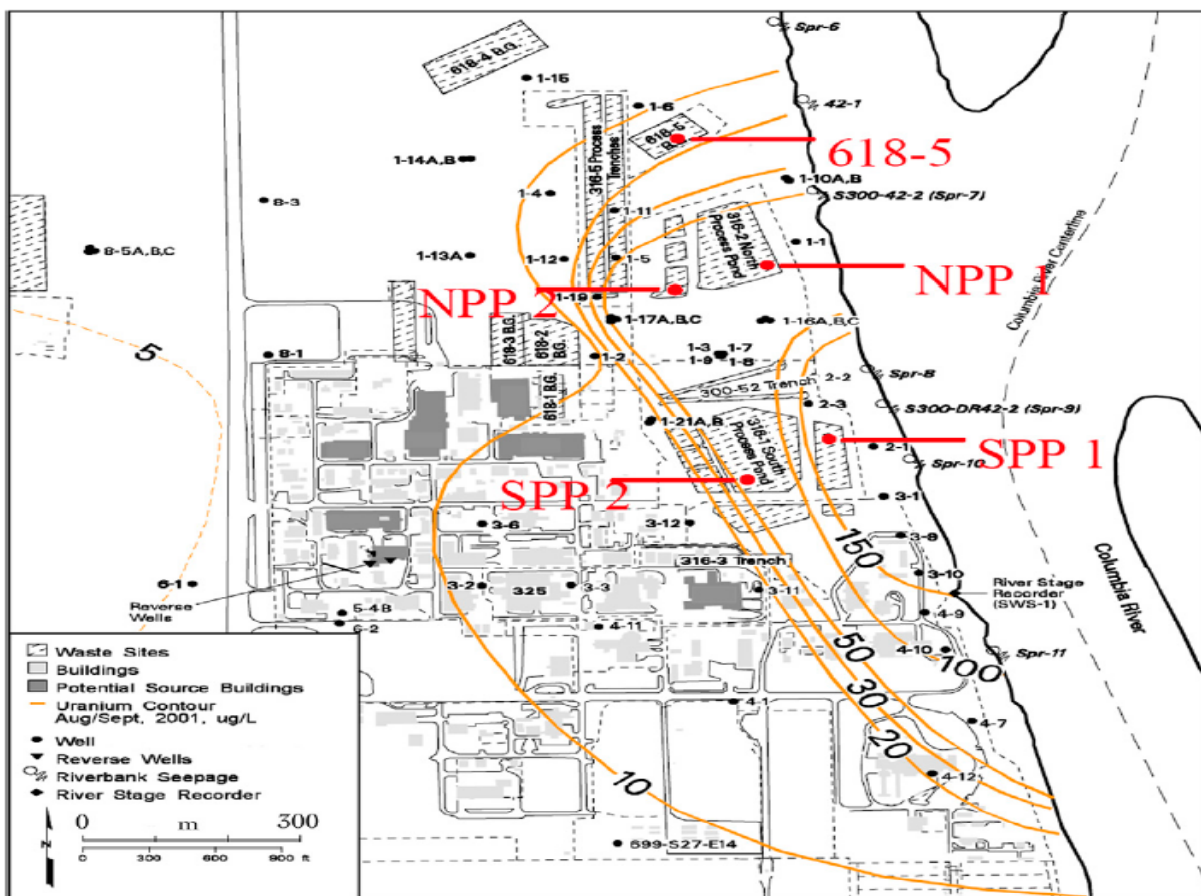
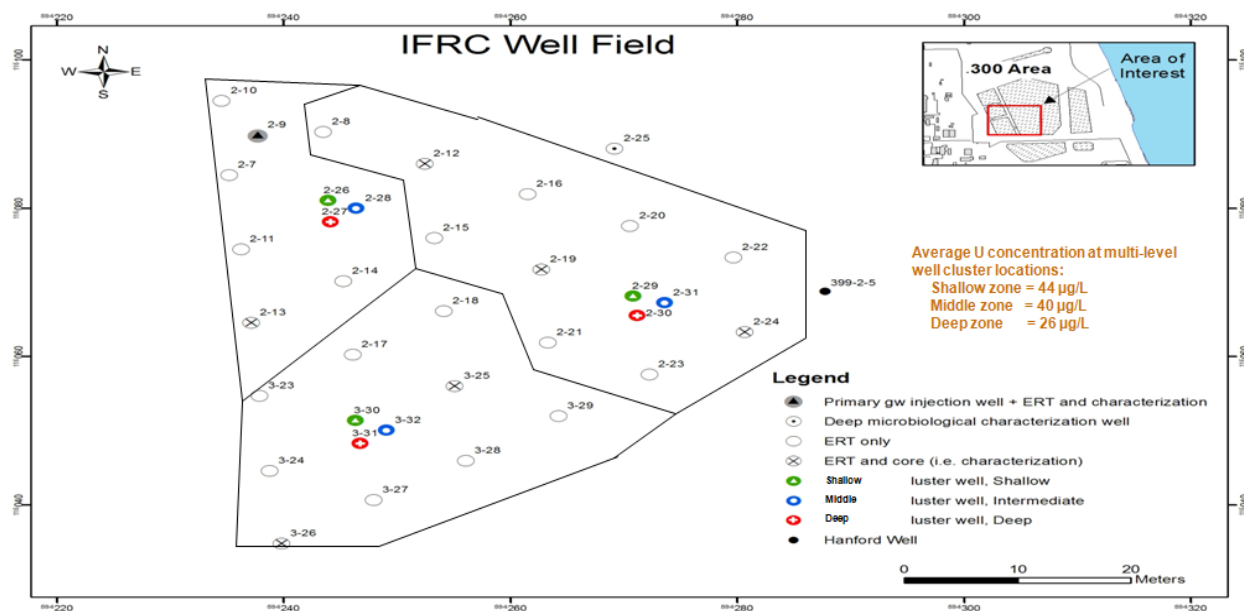


Figure 2. Uranium plume concentrations in the Hanford Site, 300 Area (Source: McKinley). The excavated process ponds were located near the river shore. The process ponds (PP) sample locations are indicated.

Not all fundamental scientific questions regarding the movement of subsurface contaminants like uranium, are answered; for example, how does the subsurface microbial community in Hanford's unconfined aquifer impact the fate and transport of the contaminant (Lin 2009)? The answers to such questions could potentially lead to new biogeochemistry knowledge and plausible bioremediation solutions for the contaminant. The groundwater uranium plume in the 300 Area of the Hanford Site exceeds the Environmental Protection Agency (EPA) drinking water standard limit 30ppb of uranium concentration. This makes this site an ideal place to both study the movement of subsurface contaminants and its microbes, especially since an experimental well field to sample the soil and groundwater there has been constructed (Figure 3). Results that can help scientists understand the processes and mobility of uranium could immediately benefit the area to control the elevated uranium concentrations.



**Figure 3. Summary of uranium and tracer response data at the Integrated Field Research Challenge (IFRC) Well Field in the south process pond.**

Furthermore, despite the uranium plume and its potential toxicity, scientists like Xueju Lin have characterized the present microbial communities in the area (Figure 4), demonstrating that different microbial strains dominate at different depths (Lin 2009). Thus, they could also all potentially be interacting and playing a role in the mobility and fate of uranium. If so, microbes could then be utilized as part of a solution for controlling the fluctuating uranium plume. However, for a strategy of this nature to succeed, an environment that stimulates microbial growth is needed to affect the normal sorption and reduction kinetics of uranium. Additionally, a high rate and extent of microbial reduction of U(VI) in the presence of ions commonly found in groundwater that can form complexes with uranyl is also required (Kelly 2005). Microbial growth is usually regulated by available or limited nutrients; although it is assumed that carbon is the most common limiting growth factor, other nutrients such as nitrogen and phosphorus can also play a role (Demoling 2007). To demonstrate, Fredrik Demoling determined that for most soils he tested, adding carbon (2.5-3 mg glucose/g of soil) increased the bacterial growth rates by 1.5-2X, while nitrogen addition tended to decrease bacterial growth rates, and phosphorus

addition had little effect, with an observed 7% mean increase in bacterial growth (Demoling 2007). However, in one particular case, the bacterial growth rates in soil increased approximately 5 times after adding phosphorus, which shows that the soil composition is also a factor. Sandy garden, Grassland, and Lake shore soil were the most responsive to having phosphorus as a limiting growth factor in Demoling's experiments. If the DOE implements soil tri-polyphosphate injection treatments to sequester uranium in the vadose zone at the Hanford site, different types of uranium phosphate minerals such as Autunite should form (Dawn M. Wellman, 2006). As a result, there is reason to believe that local microbial populations could increase and consequently multiply their biogeochemistry effects on the area. It is generally accepted that the traditional explanation of why most systems are carbon limited is because all the carbon in the soil is not available. Further, the process of recycling dead microbial biomass which releases carbon as CO<sub>2</sub> decreases the C/N ratio. Because nitrogen and phosphorous are present in such great amounts in nucleic acids and proteins, the cell requirements of these elements in bacteria are large. As a result, bacterial cells should maintain low intracellular C:N:P ratios [Tezuka 1990, Goldman et al. 1991 from Ichinotsuka 2010 paper]. The bacteria themselves also play a role in the uptake of nutrients in the soil; slow growth rates use more carbon for maintenance leaving less available for growth and biomass production. However, in aquatic systems, bacterial growth rates are faster than in soil [BATHH 1998 from Demoling 2007 paper], so it is not surprising that scientists can find them limited by lack of nutrients such as phosphorus instead of carbon [Morris and Lewis, 1992; Pinhassi et al., 2006 from Demoling 2007 paper]. Therefore, the amount of available nutrients can constrain bacterial biogeochemistry processes and growth rates [Rivkin & Anderson 1997, Caron et al. 2000, Hoch & Bronk 2007 from Ichinotsuka 2010 paper].

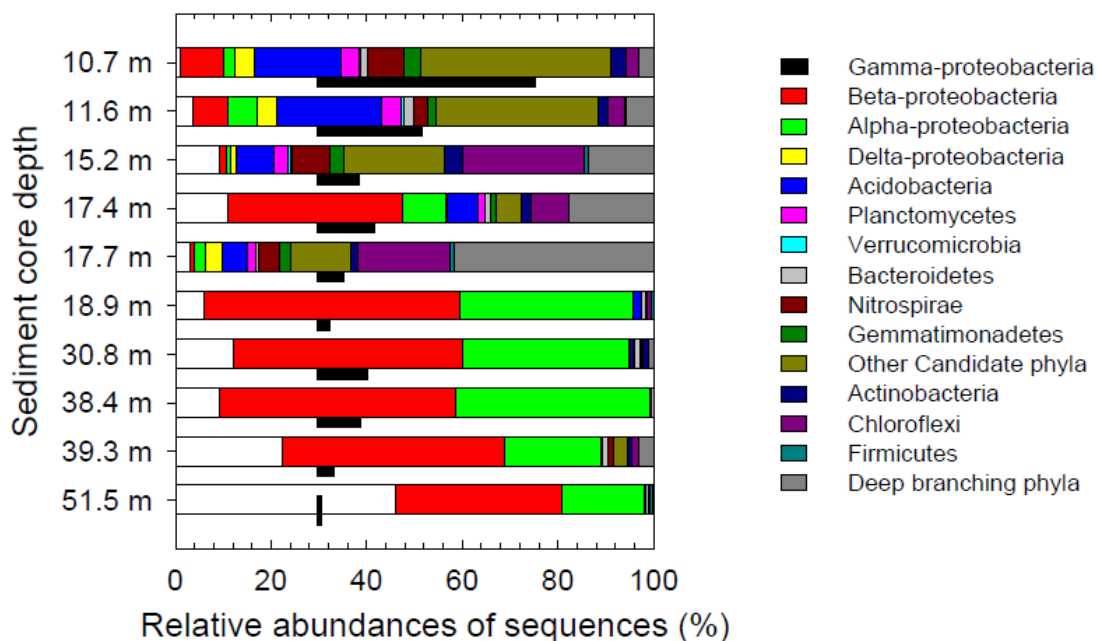


Figure 4. Relative abundance of microbial populations found in the Hanford 300 Area with respect to depth (Source: Xueju Lin).

Although the surface sources of the 300 Area uranium plume were long-since excavated and removed, a significant groundwater concentration of uranium persists and migrates to the environmentally sensitive Columbia River, particularly through the interface between groundwater and the riverbed. The persistence of the plume suggests that the Hanford formation sediments in the vadose zone provide a solid-phase source of uranium to the groundwater. All of the vadose uranium is hexavalent, which is coordinated as the uranyl ion ( $\text{UO}_2^{2+}$ ) (McKinley 2007). Thus, in theory, taking advantage of the conditions of the soil and groundwater, depending on the sorption kinetics and toxic effects of uranium on the microbiological community of the 300 Area, an effective bioremediation solution could arise to help control and reduce the uranium plume protecting the surrounding area.

## 2. THEORY

---

### 2.1 Uranium

The element uranium (U) has a standard atomic weight of 238.03 g/mol with an atomic number of 92. U exists as aqueous (mobile) and sorbed/precipitated (immobile) phases in sediments where their relative concentrations are governed by equilibrium and/or kinetic reactions of sorption/desorption and precipitation/dissolution (Liu 2007). The rapid reduction rate of oxidized U(VI) in some bacteria and the low solubility of reduced U(IV) makes this biogeochemistry process an attractive bioremediation option for removing U from contaminated groundwater which typically exists as uranyl carbonate (Brooks). At most sites, where molecular oxygen is present, most U in the aqueous phase will be in the form of the hexavalent uranyl cation  $\text{UO}_2^{2+}$ . Mobility of this cation is enhanced by short-chain fatty acids that through chelation can increase mobility (VanEngelen 2010). ASTM-A-380 defines chelating as "chemicals that form soluble, complex molecules with certain metal ions, inactivating the ions so that they cannot normally react with other elements or ions to produce precipitates." Being very soluble and possessing complex structural and speciation properties, uranium (VI) is a very difficult contaminant for mobility predictions. Aqueous uranium can easily adsorb onto soil minerals and bacterial surfaces such that its mobility and speciation in the environment are affected (Gorman-Lewis 2005). Phosphorus, pH, and carbonate are influential because in solutions above pH 5, the uranyl ion hydrolyzes, forming aqueous hydroxide complexes and polymers of uranyl hydroxide (McKinley 2007). According to Langmuir (1978), the hydroxy complexes are relatively weak, and in most groundwater's, uranyl occurs as stronger complexes with dissolved carbonate (as cited in McKinley 2007). Uranyl hydroxides may precipitate where the more soluble complexes are absent; otherwise uranyl carbonates (or sulfates) may precipitate from the uranyl complexant solution, or, where dissolved silica or phosphate are available, the relatively insoluble silicate or phosphate minerals precipitate.

The UV-VIS spectra of U(IV) species has a sharp absorption band between 600 and 700 nm, with four main peaks between 400 and 700 nm, unlike U(VI) which has one peak at 400 to 500 nm (Figure 5-a). Normally, reduction of U(VI) to U(IV) can be monitored via the UV-VIS spectra which is how we know that strong complexation agents such as citrate, NTA, and EDTA affect the chemical species (U(IV)) and its reduction rate. These organic acids can affect the sorption, precipitation, and redox behavior of U by forming stable complexes. It is well known that diverse bacteria use soluble U(VI) as an electron acceptor for respiration and reduce it to insoluble  $\text{UO}_2(\text{s})$  (Suzuki 2010). In under-saturated solutions, sorption influences uranyl ion mobility (McKinley 2010). The rapid kinetics of bacterial U(VI) reduction and low solubility of uraninite ( $\text{UO}_2, \text{cr}$ ) make this process an attractive option for removing uranium from groundwater. Nevertheless, conditions that may promote or inhibit U(VI) reduction are not well-defined (Brooks 2003) and was explored through experiments with variable concentrations of pH, and carbonate as it would also occur in the soil during future testing.

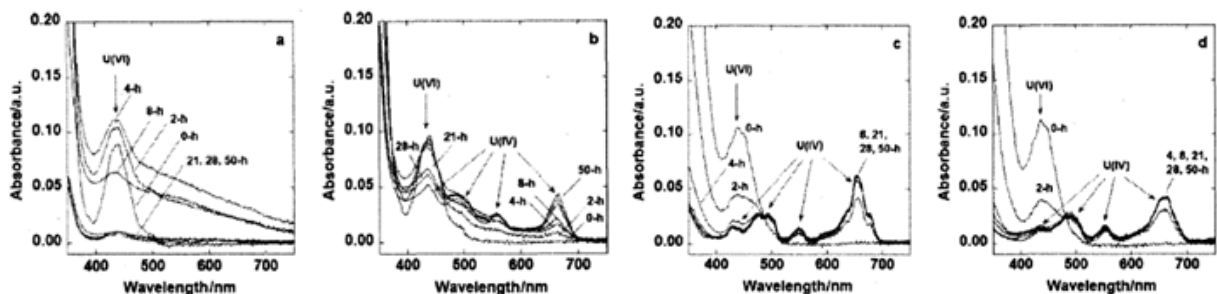


Figure 5. Typical UV-VIS spectra of the A) control, B) citrate, C) NTA, and D) EDTA media at 0, 2, 4, 8, 21, 28, and 50 hours after inoculation with *S. putrefaciens*.

### Pure culture bacterial model

Because off-site work with the microbes in the groundwater at the Hanford 300 Area is not easily accessible, work with a representative microbe from the area, an *Arthrobacter* species, was used to study its biogeochemistry role with the contaminated uranium plume. The *Arthrobacter* genus is the most common for cultures from both contaminated SX-108 and the uncontaminated 299-W22-48 boreholes in Hanford vadose sediments. These were collected from the vadose zone beneath the SX-108 tank located within waste management area S-SX at Hanford. Nineteen of the 20 radiation-resistant isolates were gram positive bacteria, 13 of which were phylogenetically related to members of *Arthrobacter* and its close relative *Micrococcus* (James K. Fredrickson). Additionally, of 40 strains of gram-positive, aerobic, heterotrophic bacteria isolated from saturated subsurface lacustrine, paleosol and fluvial sediments at the Hanford Site, 38 were closely related to *Arthrobacter*. In fact, most of the subsurface isolates were found to be most likely novel strains or species of *Arthrobacter* (Crocker 2000). Characterization by phylogenetic analysis of 16s RNA gene sequences and by determination of elected morphological, physiological, and biochemical traits confirmed this. Analyses by Balkwill et al., 1997, implied that roughly 25% of the subsurface isolates were most closely related to the genus *Arthrobacter*, making them the most numerically predominant component of the culturable aerobic microbial community from the 300 Area.

Previous studies have indicated that, in general, gram-positive bacteria such as *Arthrobacter spp.* are more drought tolerant than gram-negative organisms like *Pseudomonas spp.* In fact, *Arthrobacter* members appear to be well adapted to life in arid soils, and some members are adept at surviving for extended periods of desiccation. Members of the genus *Arthrobacter* also appear to be well adapted to vadose sediments of the Hanford Site, as approximately one third of the total isolates and a significant number of cloned sequences (11 out of 48) from a study were related to members of this genus. This is about the same proportion of total viable aerobic chemoheterotrophic bacteria as was isolated from pristine Ringold Formation sediments obtained from another location on the Hanford Site. *Arthrobacter* species were also common isolates in a third study of vadose zone sediments at the Hanford Site (Fredrickson 2000). *Arthrobacters* are considered to be ubiquitous and predominant members of culturable soil microbial communities that are widely believed to play a significant role in the transformation of organic matter in natural environments. The major fatty acids of the subsurface strains and *Arthrobacter* reference

strains were anteiso- and iso terminally branched saturated fatty acids, including 13-methylpentadecanoic acid (anteiso-C<sub>15:0</sub>), 14-ethylpentadecanoic acid (iso-C<sub>15:0</sub>) and 15-methylhexadecanoic acid (iso-C<sub>16:0</sub>) (Crocker 2000). Presently, Xueju Lin from PNNL has determined that in the south process pond in the 300 Area, the phylum *Actinobacteria*, which encompasses the *Athrobacter* genus, accounts for 15% of the microbial population on average in the oxic sediments as shown in Figure 4.

## 2.2 Microbial Adsorption Proof

It has already been demonstrated, in both laboratory and field studies conducted by numerous scientists such as Beveridge and Murray, 1976, 1980; Gonçalves et al., 1990; Konhauser et al., 1993; Fein et al., 1997; Fowle and Fein, 1999 (as cited in Fowle 2000), that bacteria effectively bind metal ions through adsorption reactions with the functional groups of the bacterial cell wall. In contrast, the uranyl cation  $\text{UO}_2^{2+}$  can be immobilized within bacterial biomass by metabolizing the cellulose and cellulosic breakdown products found in other environments (VanEngelen 2010). Therefore, bacteria have the potential to affect the mass transport and fate of aqueous metal ions through adsorption reactions in water-rock systems making it crucial to accurately and quantitatively model bacteria-metal adsorption reactions (Fowle). Generally, uranyl is complexed by negative fixed-charge or amphoteric sites on mineral surfaces. Aqueous complexation reactions, such as those with carbonate or sulfate species, compete with surfaces for dissolved uranyl and may limit the extent of the sorption reaction. The retardation and immobilization of uranium in a reactive mobile system is thus a function of the interplay between oxidation-reduction, sorption, and precipitation, affected by reactants and reactions along a groundwater flow path. It is expected that the advected uranyl in the migrating contaminant plumes to interact with solid surfaces either through sorption or precipitation (McKinley 2010).

Negatively charged uranyl complexes tend to dominate the aqueous uranium speciation in oxygen/aerobic and CO<sub>2</sub>-rich systems. However, because microbial cell wall surfaces are negatively charged, there are no great expectations of adsorption occurring at the interface; yet extensive stable uranium adsorption, in from the uranylhydroxide, uranyl-carbonate, and calcium-uranylcarbonate species have been reported onto species like the *Bacillus subtilis* bacterial cell surface (Gorman-Lewis 2005). Other examples of cells that can really uptake and desorb uranium are the indigenous *Bacillus*, *B. Cereus*, *B. megaterium* and *B. sphaericus* strains (Selenska-Pobell 1999). Theoretically, an equilibrium state exists that controls the concentration of metal associated with the bacterial surface relative to that free in solution such that regardless of whether the steady-state condition was approached from under-saturation, no metal initially associated with the bacterial surface, or from super-saturation, nearly all of the aqueous metal initially associated with the bacterial surface, the final concentration of metal bound to the bacterial surface is the same (Fowle 2000). Thus, desorption should be tested under conditions where only partial desorption occurs, comparing the extents of adsorption and desorption under identical pH and solute conditions (Fowle 2000). Previous kinetics studies with *B. subtilis* showed that steady-state adsorption can be achieved within 30 minutes and persist for at least 24 hours (Gorman-Lewis 2005). The ability of iron- and sulfate-reducing bacteria to couple oxidation of organic substrates to U(VI) reduction under anaerobic conditions plays a prominent role in many uranium bioremediation schemes. However, many contaminated sites are aerobic;

therefore,  $\text{UO}_2^{2+}$  reduction, in anaerobic processes, is not expected to play a large role in decreasing uranium mobility in these systems. Biosorption of bacteria is the most promising pathway for uranium immobilization (VanEngelen 2010).

### 2.3 Uranium Sorption & Toxicity Mechanism

Gordon E. Brown concluded that the toxicity and bioavailability of a heavy metal depends in part on reactivity and solubility, which are determined by the speciation or chemical form of the element defined as (i) the identity of the element, (ii) its oxidation state, (iii) its physical state (1999). In the same manner, the toxicity of a heavy metal to microbes depends upon its bioavailability. In natural environments microbial communities predominantly (~99%) exist as biofilms, which often possess significant capability to immobilize metals. The different mechanisms by which biofilms immobilize metals or radionuclides include: (1) biosorption to cell components or extracellular polymeric substances (EPS), (2) bioaccumulation, (3) precipitation by reaction with inorganic ligands such as phosphate, and (4) microbial reduction of soluble metal to insoluble metal (Figure 6) (Nancharaiah 2006). In a similar fashion, it was suggested that the uranium was taken up by *C. regularis* as the cation form ( $\text{UO}_2^{2+}$  or  $\text{UO}_2\text{OH}^+$ ), and *Chlorella* cells took up uranium in exchange for their protons in analogy with some organic chelating agents. In this manner, the uptake of uranium by *C. regularis* was rapid and unaffected by light, temperature, metabolic inhibitors, and reversible, as most of uranium taken up by *C. regularis* was easily released by EDTA solution. Thus, at least for *C. regularis*, the suggested uranium uptake mechanism depends upon the physical adsorption on the cell surface, but not upon the biological activity (Nakajima). Reports from Gorman-Lewis (2005) indicate that the relatively high extent of adsorption under high pH conditions is due to adsorption of the uranyl aqueous complexes themselves onto the bacterial surface. Adsorption of these negatively charged aqueous uranyl complexes onto a highly negatively charged bacterial surface is surprising and must reflect an adsorption energetic that can overcome the high forces of electrostatic repulsion between the cell wall and the aqueous uranyl complex. Also, they suggest that neutrally and negatively charged uranylhydroxides, uranyl-carbonates, and the calcium-uranylcarbonate complex form highly stable surface complexes on the negatively charged *B. subtilis* surface, leading to significantly enhanced adsorption in the pH range of 7-9. Clearly, electrostatic interactions alone cannot account for the observed adsorption behavior. Some other driving force for the adsorption, such as that of covalent bonding, from species such as uranyl-carbonate, must also be present for highly negatively charged aqueous complexes to adsorb onto the negatively charged bacterial surface to the extent observed by Gorman-Lewis. Additionally, Nancharaiah (2006) observed that cations such as  $\text{Na}^+$ ,  $\text{K}^+$ ,  $\text{Mg}^{+2}$ , and  $\text{Ca}^{+2}$  were simultaneously released into the bulk solution during U(VI) biosorption with dead or live bacteria, indicating there is involvement of a passive ion exchange mechanism in radionuclide uptake. The amount of metal ions released was in the order  $\text{K}^+ < \text{Ca}^{+2} < \text{Mg}^{+2} < \text{Na}^+$ . Such metal ion release was analyzed by flame photometry or atomic absorption spectrophotometry. We must closely look to see if the length of adsorption contact time exhibits any effect on the kinetics of desorption or on the concentration of metal associated with the bacterial surface after desorption. If it does not affect it, we can suggest that the sorption sites are located at or very close to the bacterial surface and that uptake of the metal into the interior of the cell is negligible under non-metabolic experimental conditions. Previous studies demonstrate that the protonation and deprotonation of the cell wall functional groups is a fully reversible process (Fowle 2000). Further, carbon-free

and heat-killed controls accumulated the least amount of  $\text{UO}_2^{2+}$ . This suggests that actively metabolizing cells accumulate significantly more  $\text{UO}_2^{2+}$  (VanEngelen 2010). As an example, U was not removed by heat killed *Desulfovibrio desulficans* cells (Sani 2006). Considering the negative zeta potential of bacteria reveals that positively charged  $\text{UO}_2^{2+}$  complexes will be electrostatically attracted to the surface of the negative charged cells. Recent experiments with *Pseudomonas aeruginosa* (ATCC 10145) showed that starved and dead cells had more negative zeta potentials compared with metabolically active cells. This difference may explain why starved and killed cells, like those in the oligotrophic conditions at the Hanford Site, could accumulate more positively charged species and be less susceptible to toxic effects of negative charged uranium species (VanEngelen 2010).

The toxic effects of U(VI) can affect the cells in multiple ways: inhibition of total cell protein, decrease in U(VI) reduction rates, longer lag times, and in some cases, no measurable growth. It has been shown that the toxicity of a metal depends on solubility, speciation, and chemical properties as well as on geochemical factors such as complexation, pH, and precipitation (Sani 2006). Toxicity is believed to result from displacement and/or substitution of essential ions from cellular sites and from blocking functional groups of important biochemical molecules, such as enzymes, polynucleotides, and essential nutrient transport systems (Sani 2006). This can cause denaturation and inactivation of enzymes as well as disruption of cell organelle-membrane integrity. For U in particular, it has been shown under laboratory conditions that some bacterial species can use U(VI) as a terminal electron acceptor. No facilitated diffusion of metal bound to an assimilable ligand such as uranium phosphate complex was found in alga (Fortin 2004).

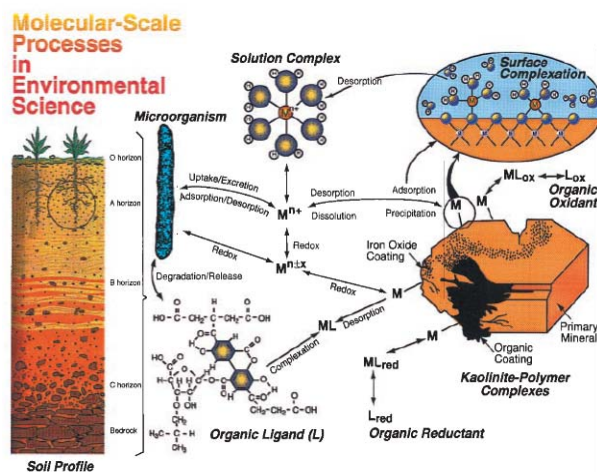


**Figure 6. Schematic illustration of a variety of molecular environmental science processes affecting contaminant elements in soils and ground water (Source: Gordon E. Brown).**

Enzymatic reduction of U(VI) to U(IV) has been suggested as the primary microbial detoxification mechanism (Sani). It has also been suggested that to have a physiological or toxic effect, most heavy metals have to enter the cell; yet, in the study conducted by Sani (2006), TEM showed that in the less toxic bicarbonate buffer, more U entered the cells compared to the medium without bicarbonate. In general, the mechanism of U(VI) toxicity and inhibition in microbiological systems are not understood. U(VI) is able to react with electron-transfer

proteins localized in the periplasm, where after accepting electrons, precipitates as uraninite due to its low solubility. Because the cytoplasmic membrane would act as a barrier, it is most likely that any reduced solid phase U found in the cytoplasm is also due to U(VI) reducing activity in the cytoplasm (Figure 7) (Sani 2006). The periplasmic protein cytochrome C3 has been determined to play a role in providing electrons for U(VI) reduction in *D. desulfuricans* G20, but other proteins are likely to play a significant role as well (Sani 2006). Fortin (2004) found no evidence that uranium could cross biological membranes as the uranium–phosphate complex via a phosphate transporters and facilitated diffusion in green alga, but it remains a possibility. The prevailing paradigm for metal uptake by aquatic organisms (i.e., the free ion activity model or its derivative, the biotic ligand model) assumes that metals enter living cells via facilitated cation transport (Fortin 2004).

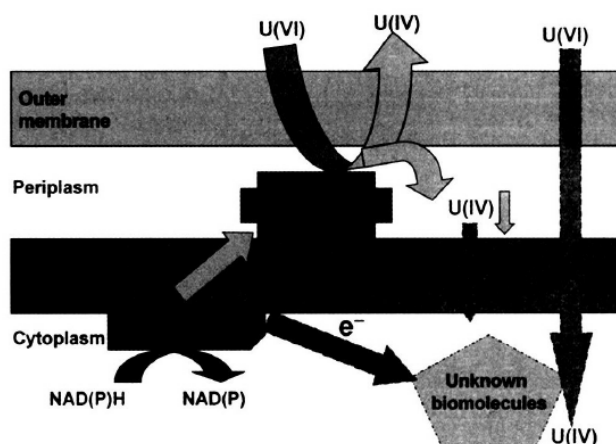


**Figure 7. Uranium detoxification model in *Desulfovibrio desulfuricans* G20. NAD(P)H = reduced form of nicotinamide adenine dinucleotide phosphate; U(VI) = reduced uranium; U(IV) = uranium (VI) (Source: Sani).**

## 2.4 Effects of pH

Variable alkalinity is the primary chemical control on U adsorption (Zachara 2009). It is well known that, when looking at desorption isotherms, complete solute desorption is promoted by drastically changing system conditions, such as lowering the solution pH to 2 or lower as studied by Harvey and Leckie, 1985, Manmaril et al., 1997, or introducing a strong chelating agent such as EDTA studied by Puranik et al., 1995 (as cited in Fowle 2000). Thus, we know to expect desorption to occur under these conditions as pH will play a very important role in the fate of uranium speciation in the environment. For example, above pH 5, neutral and negatively charged uranyl-carbonates dominate the aqueous uranium speciation significantly reducing uranium adsorption onto minerals (Gorman-Lewis 2005). Moreover, for groundwater systems where high calcium concentrations are common, the aqueous calcium-uranyl-carbonate complex can dominate, making it less available for adsorption (Gorman-Lewis 2005). Electrophoretic mobility measurements of *B. subtilis* cells demonstrate that the bacteria exhibit a negative surface charge above pH 2, with increasing negative charge with increasing pH (Gorman-Lewis 2005). These observations are consistent with successive deprotonation of bacterial surface sites

with increasing pH and suggest that neither  $\text{Na}^+$  from the electrolyte nor elements such as Ca and Mg that may be released to some extent from the cell wall significantly affect the bacterial surface charge under the conditions of the experiments (Gorman-Lewis 2005). Furthermore, the increasing negative charge should aid in the affinity of bacterial cell wall for free positive uranyl species. However, amounts of uranium sorbed by the granular biomass at pH 4.0 and 7.0, in the long run, after 24 hours of incubation are not significantly different, suggesting that initial pH influences the rate of uranium biosorption, which can be almost complete within an hour (max 218 mg/g for granular biomass), but not the total U sorption (Figure 8) (Nancharaiah 2006). It is also suggested that cells can take up uranium in exchange for their protons in analogy with some organic chelating agents, much like *Chlorella* cells, according to the following equation (L means algal cells as ligands):  $\text{LH}_2 + \text{UO}_2^{2+} \rightleftharpoons \text{LUO}_2 + 2\text{H}^+$ . In the low pH region, the formation of  $\text{H}^+$  was depressed and the equilibrium was shifted to left, and then the amounts of uranium taken up by *Chlorella* cells decreased (Nakajima 1979). Thus, acidic pH ranges induced faster biosorption compared to that at pH 7 or above (Nancharaiah 2006).

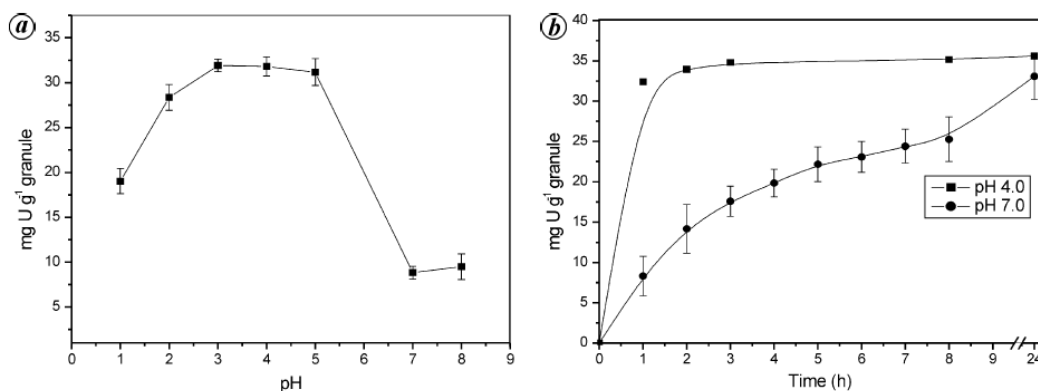


**Figure 8. Effect of pH on removal of soluble uranium u(VI) by granular biomass. A) U(VI) uptake at different initial pH values determined after 1 h contact time. B) Time course of u(VI) biosorption at pH 4 and pH 7 (initial (U(VI)) concentration: 100 mg/L, error bars : ±1SD. (Source: Nancharaiah)**

## 2.5 Effects of Phosphate

The Nakajima group (1979) determined that the uptake of uranium was hindered by phosphate and carbonate ions and was not affected by cations (sodium, potassium, ammonium, magnesium, calcium, manganese, cobalt, nickel, and zinc ions), nitrate, sulfate, and thiosulfate ions. The amounts of uranium taken up by *C. regularis*, the microbe they tested on, rapidly decreased with increasing the concentration of phosphate ion in the uranium solution. Thus, simulations of phosphate amendment treatments, as can be anticipated by any tri-polyphosphate injection remediation work, should be conducted with the microbes in question to determine if it will inhibit any uptake of uranium by the microbes. In Lake Dillon, a mesotrophic Colorado reservoir, population growth rates were highly correlated with phosphorous concentrations but not with dissolved organic C concentrations. Bacterioplankton growth in the summer epilimnion responded strongly to the addition of P alone or in combination with N or labile organic C. The field data in the Colorado reservoir shows that bacterioplankton are frequently without sufficient nutrients to sustain maximum growth; the experimental and statistical analysts indicate that P, rather than organic C, is the critical nutrient for bacterioplankton growth in this lake (Morris

1992). As such, the predicted increased bacterial population or growth rates due added phosphate should be tested and confirmed that at the current levels, will not interfere with any sorption phenomena. High concentrations of phosphate (1.5-5mM) was sufficient to inhibit U toxic effects on some bacteria (Sani). Phosphate is known to directly precipitate U(VI) phosphate complexes (Sani 2006). Complexation of a metal by a ligand such as phosphate is expected to decrease its bioavailability and thus its toxicity. Phosphate, citrate, or EDTA reduces uranium's bioavailability; The binding of the U by phosphate (e.g.,  $\text{UO}_2^{2+} + \text{HPO}_4^{2-} \leftrightarrow \text{UO}_2\text{HPO}_4^0$ ;  $\log K=7.24$ ) will reduce the free  $\text{UO}_2^{2+}$  concentration and thus, according to the FIAM/BLM, 2 should reduce uranium bioavailability (Fortin 2004). Inorganic elements other than phosphorus have been shown not to affect microbial growth in drinking water. The addition of phosphorus (50 ug of  $\text{PO}_4\text{-P}$  liter<sup>-1</sup>) increased microbial growth in fresh drinking water produced from surface water or groundwater. Even the addition of 1 mg of phosphate phosphorus increased the microbial growth. The addition of phosphorus to surface and groundwater samples greatly increased the growth of heterotrophic bacteria. Phosphorus has a major ecological role in nature, because it is an essential element for microbes and because it is commonly the least abundant element compared to carbon (Miettinen 1997).

## 2.6 Effects of Carbonate

Results of the compositions of the chemical species of aqueous U(VI) in the carbonate solution suggested that carbonate ion formed a stable complex ions with uranyl ion, such as  $\text{UO}_2(\text{CO}_3)_2^{2-}$  or  $\text{UO}_2(\text{CO}_3)_3^{4-}$ , and other uranyl carbonate complexes which were not taken up by *C. regularis* (Nakajima 1979). In fact, given enough carbonate, like in the form of sodium hydrogencarbonate, < 0.0102 M, and the uranium uptake can be reduced to zero as in the case of both living or scalded *Chlorella* cells (Nakajima 1979). Uranyl ion forms very stable complexes with the carbonate ion that does not allow it to be bio-available to the cell. Phillips et al. reported that U(VI) reduction by *D. desulfuricans* decreased as the concentration of bicarbonate was increased from 30 to 100mM (Brooks 2003).  $\text{UO}_2^{2+}$  accumulation is significantly more in low bicarbonate concentrations; however, growth inhibition and bioaccumulation varied depending on the growth substrate. This increase accumulation in low levels of bicarbonate is due to  $\text{UO}_2^{2+}$  aqueous complexation, the presence of positively charged and unstable  $\text{UO}_2^{2+}$  hydroxide complexes explain the greater sensitivity and ability to accumulate. In contrast, the negatively charged and stable  $\text{UO}_2^{2+}$  carbonate complexes in the high bi-carbonate medium has less interaction with the bacteria (VanEngelen 2010). In carbonate buffer (30 mM, pH 7), *D. desulfuricans* strain Essex6, G20, and *Desulfovibrio* sp. Strain UFZ B did not exhibit any toxic effects in U(VI) concentrations up to 5, 2, and 1 mM, respectively (Sani 2006). With this carbonate buffer, U(VI) is almost entirely complexed as  $\text{UO}_2(\text{CO}_3)_2^{2-}$  (15%) and  $\text{UO}_2(\text{CO}_3)_3^{4-}$  (85%).

## 2.7 Effects of Calcium

According to Serne et al., 2002, Calcium is a common chemical component in groundwater and has a concentration range of 0.5–50 mmol/L and a medium of about 5 mmol/L in the Hanford pore water and groundwater (as cited in Liu 2007). Calcium is a common ion in groundwater that can complex with U(VI) in bicarbonate solutions to form a ternary calcium-uranyl-carbonate species  $[\text{Ca}_2\text{UO}_2(\text{CO}_3)_3(\text{aq})]$  (Bernhard et al., 1996, 2001; Kalmykov and Choppin, 2000 from Liu 2007 paper). Speciation calculations and spectroscopic analyses indicated that either

$\text{UO}_2(\text{CO}_3)_3^{4-}$  or  $\text{Ca}_2\text{UO}_2(\text{CO}_3)_3$  could dominate the aqueous U(VI) speciation depending on the chemical composition, pH, and calcium concentration in the Hanford pore and groundwaters (Dong et al., 2005; Wang et al., 2004) from Liu 2007 paper). Microbial reduction of U(VI) has also been shown to be inhibited by Ca in solution, due to indirect evidence that the Ca-UO<sub>2</sub>-CO<sub>3</sub> complex is also less bioavailable to the microbes (Kelly 2005 and Liu 2007). In some instances, the overall rate of microbial reduction of solid phase U(VI) was limited by U(VI) dissolution reactions in solutions without calcium and limited by microbial reduction in solutions with calcium (Liu) (Brooks). Calcium and dissolved CO<sub>2</sub> are ubiquitous components of natural and contaminated groundwater (Brooks 2003). Possible causes for the inhibition of U(VI) reduction in the presence of Ca include: (i) the complexation of lactate or carbon source by Ca making it less bioavailable as an electron donor, (ii) a direct physiological effect of Ca on the cells that inhibited U(VI) reduction, [When the concentration of Ca was 5 mM, there was a substantial lag phase prior to the onset of U reduction, so inhibition was independent of the electron donor, so this might be the cause] or (iii) the formation of an aqueous Ca- U-CO<sub>3</sub> complex that was less susceptible to enzymatic reduction by CN32 (Brooks 2003). Equilibrium speciation calculations suggest that calcium may increase the solubility of solid phase U(VI) at circumneutral to alkaline pH, resulting from the effect of calcium on U(VI) aqueous speciation. The increase of the solubility may increase the bioavailability of solid phase U(VI) as suggested by a recent study showing that solid phase U(VI) has to dissolve before it is bioavailable for microbial reduction (Liu et al., 2006a as cited in Liu 2007). However, whether or not the solubility increase will also increase the rate of U(VI) dissolution (Liu et al., 2006b as cited in Liu 2007) and thus may enhance the overall rate of microbial reduction of solid phase U(VI) (Liu 2007) has to be experimentally determined to our 300 Area microbes.

### 3. RESEARCH DESCRIPTIONS

#### 3.1 Cell Preparation

For the uranium toxicity assays with the Leucine Incorporated Method, 500 ml of groundwater was collected from the Integrated Field Research Challenge (IFRC) groundwater wells in the South Process Pond of the 300 Area: the deep well, channel 5, 2-27; the shallow well, channel 6, 2-26; and the shallowest well, 3-23, where water had to be bailed out. Then, 100 ml of this groundwater was filtered sterilized using a 0.1 micron filter paper and re-suspended in 100 ml of synthetic groundwater (SGW) that has no carbonate or uranium, unlike the pure groundwater. Recovery from the filtering method can range from 25-100% of cells, the final concentration of cells utilized were analyzed with fluorescent microscopy methods.

Because of problems of overestimating the number of viable bacteria when direct microscopic methods are used and of underestimating the number of viable cells when culture methods of enumeration are used, an average of both, or a scientifically sound estimate should be used. Comparison of results of plate counts, direct microscopic enumeration, and indirect activity measurements indicate that the number of viable bacteria (i.e., those capable of forming colonies on a solid medium) is smaller than the number of bacteria detectable by direct microscopy by several orders of magnitude (Figure 9) (Roszak 1987).

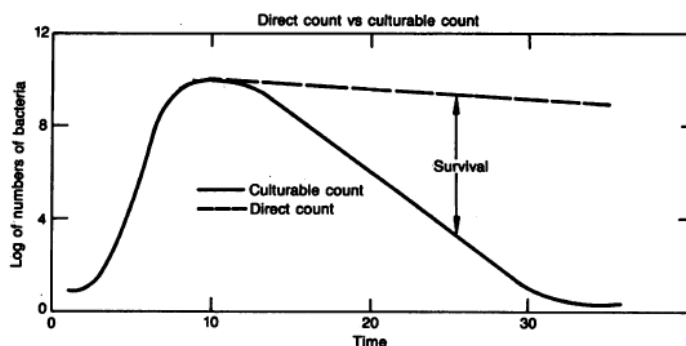


**Figure 9. Survival of the culturable population with time, including the die-off portion of the population. Typical direct count enumeration data are also shown. The difference between direct and culturable counts represents the population that remained viable but not culturable by routine or standard microbiological methods (Source: Roszak).**

#### 3.2 Synthetic Groundwater

Synthetic groundwater was made up from available salts. These compounds were chosen to duplicate the natural groundwater composition from water collected at an excavation above the former South Process Pond. The composition of South Process Pond, Pit 1 (SPP-P1) groundwater was collected for analysis on April 19, 2003, and presented by Steven C. Smith and John M. Zachara from: Groundwater Sampling and Characterization of 300-FF-5 Uranium Plume Sediments and Groundwaters on May 10-11, 2004, at Pacific Northwest National Laboratory (Table 1).

An addition of sodium and chloride in slight excess of the natural composition was allowed to avoid the problematic dissolution of sparingly soluble  $\text{CaCO}_3$  or  $\text{MgCO}_3$  (Table 2). The salts

added to de-ionized water readily dissolved, and the pH of the SGW was close to the natural value. SGW may be made up by the addition of salts directly to de-ionized water (Table 3), or by the preparation of concentrated stock solutions for later pipetting into de-ionized water. The SGW from a concentrated stock solution was prepared by three solutions A, B, and C described in (Table 4) by dissolving the masses of salts shown in 1 L of water in a volumetric flask. Weighing to the nearest 1/10th of a g is sufficient. To 800 ml – 900 ml of de-ionized water, add 10 ml of Stock Solutions A, B, and C. Stir, then bring the total volume up to 1000 ml (Table 4). However, effects of carbonate on uranium toxicity were studied using a filter sterilized carbonate-free synthetic groundwater described in Table 5.

Additionally, in order to study the uranium species formed in the synthetic ground water and in all the treatments in our experiments, MINTEQA2 modeling of uranium speciation was performed. MINTEQA2 is an equilibrium speciation model that can be used to calculate the equilibrium composition of dilute aqueous solutions in the laboratory or in natural aqueous systems. The original MINTEQ was developed at Battelle Pacific Northwest Laboratory (PNL) by combining the fundamental mathematical structure of MINEQL, a derivative of REDEQL, with the well-developed thermodynamic database of the U.S. Geological Survey's WATEQ3 model. This modeling tool allowed us to modify our treatments by knowing how much of a compound such as  $\text{HCO}_3^-$  should be added to achieve certain concentrations of uranium carbonate complexes. The software takes into account if any precipitates would form out of solution.

**Table 1. Groundwater Composition and Uranium Speciation**

	618-5 Pit 1 (26 Feb, 03)	618-5 Pit 1 (29 May, 03)	618-5 Pit 2 (26 Feb, 03)	SPP Pit 1 (19 Apr, 03)	SPP Pit 2 (19 Apr, 03)	NPP Pit 1 (26 Apr, 03)	NPP Pit 2 (26 Apr, 03)	Range
pH	7.71	8.11	7.80	7.83	8.04	7.83	7.88	7.71 - 8.11
Ionic Strength (mmol/L)	7.5	8.2	7.5	3.5	4.9	5.2	6.3	3.5 - 8.2
<b>Cations (mmol/L)</b>								
Ca	1.31	1.17	1.24	0.60	0.90	1.01	1.14	0.60 - 1.31
K	0.16	0.20	0.16	0.07	0.09	0.07	0.06	0.06 - 0.20
Mg	0.58	0.49	0.56	0.21	0.28	0.34	0.40	0.21 - 0.58
Na	1.34	2.65	1.53	0.77	0.95	0.84	1.14	0.77 - 2.65
<b>Anions (mmol/L)</b>								
$\text{Cl}^-$	0.84	1.21	0.76	0.14	0.36	0.36	0.39	0.14 - 1.21
$\text{NO}_3^-$	0.42	0.53	0.40	0.36	0.40	0.29	0.43	0.29 - 0.53
Inorg. C	2.47	2.71	2.41	1.20	1.70	2.02	1.58	1.20 - 2.71
$\text{SO}_4^{2-}$	0.69	0.76	0.85	0.35	0.43	0.47	0.88	0.35 - 0.88
$\text{Si}_{\text{Total}}$	0.57	0.59	0.55	0.28	0.39	0.32	0.23	0.23 - 0.59
<b>U (<math>\mu\text{mol/L}</math>)</b>	4.96	1.39	1.82	0.30	0.36	0.30	1.07	0.30 - 4.96
<b>Species</b>	(%)	(%)	(%)	(%)	(%)	(%)	(%)	
$\text{UO}_2(\text{CO}_3)_2^{2-}$	5.8	2.8	5.4	22.0	6.2	7.1	7.3	
$\text{UO}_2(\text{CO}_3)_3^{4-}$	3.5	5.0	4.0	6.5	4.7	4.0	3.9	
$\text{Ca}_2\text{UO}_2(\text{CO}_3)_2^0$	90.6	92.2	90.5	70.4	88.9	88.7	88.6	
$\text{P}_{\text{CO}_2}$	-2.559	-2.912	-2.656	-2.971	-3.035	-2.754	-2.913	

**Table 2. Comparison of SPPP1 Natural and Synthetic Groundwater**

	SPP Pit 1 GW	SPP Pit 1 GW	SPP Pit 1 GW	SGW	SGW	SGW	SGW minus SPP Pit 1 GW	SGW minus SPP Pit 1 GW
<b>pH</b>	7.83			8.1				
	mmol/L	mg/L	meq/L	mmol/L	mg/L	meq/L	Diff, mg/L	Diff, mm
<b>Ca</b>	0.6	24	1.2	0.6	24	1.2	0	0
<b>K</b>	0.07	2.7	0.07	0.07	2.7	0.07	0	0
<b>Mg</b>	0.21	5.1	0.42	0.21	5.1	0.42	0	0
<b>Na</b>	0.77	17	0.77	1.38	32	1.38	+15	+0.61
<b>Cl</b>	0.14	5.0	0.14	0.84	40	0.84	+35	+0.70
<b>NO3</b>	0.36	22	0.36	0.36	22	0.36	0	0
<b>HCO3</b>	1.2	73.2	1.2	1.17	17	1.17	-1.8	-0.03
<b>SO4</b>	0.35	34	0.70	0.35	34	0.70	0	0

**Table 3. Specific Salt Additions to Produce 1L of Synthetic Groundwater (SGW-SPP1)**

Salt	SGW-SPPP1 mg/L	Salt, Molecular Wt	Solubility, g/100ml
KHCO <sub>3</sub>	7.0	100.1	32.2
MgSO <sub>4</sub>	25.2	120.2	"good"
Ca(NO <sub>3</sub> ) <sub>2</sub> ·4H <sub>2</sub> O	42.4	236.15	121
CaCl <sub>2</sub> ·2H <sub>2</sub> O	61.7	147.02	"very good"
Na <sub>2</sub> SO <sub>4</sub>	19.9	142.1	"very good"
NaHCO <sub>3</sub>	92.4	84.0	7.8

**Table 4. Stock Solutions for SGW-SPPP1.**

Stock Solution	Salts	Salt, g L <sup>-1</sup>
<b>A</b>	KHCO <sub>3</sub>	0.70
	NaHCO <sub>3</sub>	9.24
<b>B</b>	Na <sub>2</sub> SO <sub>4</sub>	1.99
	MgSO <sub>4</sub>	2.52
<b>C</b>	Ca(NO <sub>3</sub> ) <sub>2</sub> ·4H <sub>2</sub> O	4.24
	CaCl <sub>2</sub> ·2H <sub>2</sub> O	6.17

**Table 5. Carbonate Free Synthetic Groundwater**

Synthetic GW for U toxicity studies (pH 7.8)

**Synthetic, CO<sub>3</sub>-free, w/ HEPES (SGW, no CO<sub>3</sub>)**

Salt	SGW mg/L	SGW g/L	Salt, Molecular Wt	conc (mM)	10x SGW g/L
CaCl <sub>2</sub> ·2H <sub>2</sub> O	88.21	0.0882	147.02	0.60	0.8821
MgCl <sub>2</sub>	19.99	0.0200	95.21	0.21	0.1999
KCl	5.22	0.0052	74.55	0.07	0.0522
HEPES, monosodium	520.58	0.5206	260.29	2.0	5.206
HCl, 0.5 M					15.4 ml

Reference solution

pH	6.8-7.0
	mmol/L
Ca	0.60
K	0.07
Mg	0.21
Na	2.00
Cl	1.69
PIPES	2.00

### 3.3 Nutrient Limiting Factor

To test the hypothesis that phosphorous injections to the soil would increase the microbial community in this area, as would possibly be the case with the tri-polyphosphate injection remediation strategy, microbial growth will be monitored after nutrient additions to the soil. Additions of C (0.046 mM acetate, 0.031 mM lactate, 0.015 mM glucose), N (0.033 mM NH<sub>4</sub>Cl, and P (0.0032 mM Na<sub>2</sub>HPO<sub>4</sub>) to sediment/groundwater slurry (0.3 g sediment, wet weight, per ml groundwater) in all possible combinations will be tested on two different types of soils in the Hanford 300 Area.

### 3.4 Uptake Kinetics & Biosorption

For future biosorption experiments, in order to ensure that the cell walls of the bacteria are stripped of competing metals and anions from the growth medium, a wash in 1mM EDTA for 1 h with 0.1M NaClO as an electrolyte should be implemented, although integrity of the cell walls after the wash procedure should be monitored using microscopy (Fowle 2000). Otherwise, the total concentration of metals in the system would be unknown, and the equilibrium states could not be calculated because the mass balance constraints would be unknown. Biosorption or removal of U(VI) from solutions should be examined under non-growth conditions, defined as

the absence of nitrogen, phosphorous, vitamins, and other micronutrients (Sani 2006). In addition, experiments should be conducted with low cell densities (~50,000 cells/ml) to minimize metal depletion through uptake and adsorption by the cells (e.g., dissolved uranium concentration bulk depletion of 5% after 60 min). Loosely bound  $^{233}\text{U}$  should be removed from the cells surface by rinsing with a supplemented 50 mM  $\text{Na}_4\text{EDTA}$ . This fraction is operationally defined as the intracellular uranium fraction and the adsorbed fraction of uranium was calculated from the total measurement (no rinse) and intracellular content (EDTA rinse) (Fortin 2004). Cells should be allowed to resume growth before implementing uranium treatment.

First, both uranium adsorption and absorption were measured after 0, 15, 30, 45, and 60 min of exposure to a total U concentration of 200 nM for example of ideal isotherm (Figure 10). The objective is to verify that uptake was linear on a short timescale. It is expected that adsorption reaches a rapid steady state, whereas absorption would steadily increase over the 60-min timeframe. For the zero-time ( $t = 1$  min) control, if uranium uptake is significantly different than zero, it could indicate that part of the surface-bound metal is not removed by the EDTA wash, and one can consider increasing its concentration. The 50 mM EDTA concentration was nevertheless selected to both maximize uranium complexation and minimize Ca/Mg complexation. Indeed, excess EDTA will virtually eliminate  $[\text{Ca}^{2+}]$  and  $[\text{Mg}^{2+}]$  in solution and at the membrane surface, thus increasing the net negative charge and electrostatic repulsion between negatively charged phospholipids, which results in greater membrane permeability if not in disruption of the membrane [29]. Part of the adsorbed uranium thus is very strongly bound to the surface, and seems to adsorb more rapidly than it desorbs, suggesting that part of the uranium surface binding is quasi-irreversible (Fortin 2004).

After the sample reaches the desired time or equilibrium, the U concentrations in filtered samples (0.1  $\mu\text{m}$ ) were measured with a kinetic phosphorescence analyzer (KPA, ChemChek Instruments). Cells were then centrifuged (6,000 g for 5 min) and washed five times with a 100  $\mu\text{M}$  EDTA (pH 5.5) solution to remove loosely bound U. Cells were then digested in 50%  $\text{HNO}_3$  and  $\text{UO}_2^{2+}$  concentrations were measured with a KPA. Cell-free, heat-killed cells (exposed to 80°C for 15 min), U-free, and carbon-free controls served as comparisons (VanEngelen 2010). Intracellular distribution of uranium within the algal cells was estimated by disrupting the plasma membrane using an ultrasonic probe (Fisher Bioblock Scientific, Paris, France). Cells were exposed for 30 min at pH 5 in the presence of 200 nM  $^{233}\text{U}$  and subsequently sonicated for 6 min (60 W; pulsed for 6 s every 7 s) in simplified culture medium containing 50 mM EDTA (to prevent freed cytosolic uranium binding to the cellular debris). The disrupted cells were then centrifuged at 100,000 g for 30 min at 15°C to separate the insoluble fraction (pellet) from the cytosol (supernatant). Though the latter was simply evaporated and the uranium redissolved with 1 ml of 1% v/v  $\text{HNO}_3$  prior to scintillation counting, the pellet was mineralized as outlined earlier for the harvested cells (Fortin 2004).

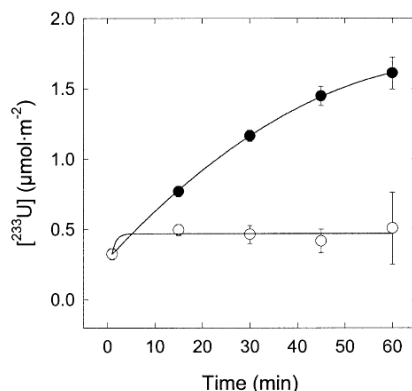


**Figure 10. Time-dependence of uranium uptake at a total concentration of 200nM (Black dots->intracellular; white dots->Extracellular). Error bars n=3. (Source: Fortin)**

### 3.5 Test Chamber/ Bioreactor

It has been reported in some studies that control experiments using polypropylene reaction vessels showed significant uranium loss from solution with starting concentrations above 4.2  $\mu\text{M}$  or about 0.952 ppm; the same was not found to be true for experiments run in Teflon reaction vessels (Gorman-Lewis 2005). A slight decrease in soluble U(VI) concentration in controls might have resulted from the adsorption of U(VI) to the glass serum bottles. It has been reported that sorption of heavy metals to serum bottles may reach 4 to 6% in the pH range of 6 to 7.5. This is also reported by Franklin Nm: “pH dependent toxicity of copper and uranium to tropical freshwater alga” (*Chlorella* sp. *Aquatic Toxicol.* 48:375-389), and Arnold T: “Sorption of U(VI) onto phylite” (*Chemical Geology*, 151:129-141) (Sani 2006). Solutions by Fortin (2004) were prepared in fluorinated ethylene propylene copolymer (Teflon) containers to minimize losses due to adsorption to container walls observed with other types of polymers (polypropylene, polyethylene). In short, adsorption of uranium to the test chamber must be tested prior to experiments.

### 3.6 Modeling

Ultimately, all parameters from experimental work should be come together to accurately model the biogeochemistry processes of uranium, proving our understanding of its mobility and fate as it interacts with all elements of its environment. The parameters needed as they relate to the effect of microbes are not limited to sorption isotherms, uranium speciation, uranium toxicity, microbial growth and activity, etc., as a function of the most important variables such as pH, carbonate, and uranium concentrations.

#### *Sorption Modeling*

Sorption isotherms are used to determine the sorption parameters of a particular microbial species such that when it is coupled with the parameters from the 300 Area soil (Table 6), and groundwater, improved models for uranium mass transport can be implemented for estimations and predictions of its fate and mobility in the contaminated area. An accurate prediction of the fate and transport of U(VI) during microbial reduction requires coupled models of geochemical and microbial processes (Liu 2007). The mobility of uranium is a complex function of the chemical and physical properties and the geological and lithological variations in the subsurface

(McKinley 2007). The model by Gorman-Lewis (2005) implements bacteria adsorption using proton active sites and chemical formulas; however, the model underestimates the extent of adsorption dramatically at higher pH values. This is strong evidence that uranyl-carbonate species, which dominate uranyl speciation under these higher pH conditions, adsorb onto the bacterial surface and are responsible for the enhanced adsorption relative to the estimated amount.

When it comes to the sorption isotherms, Nancharaiah (2006) found that the Redlich-Peterson model, ( $r^2 = 0.98$ ), gave the best fit when the experimental data were analysed using different adsorption isotherm equations (Figure 6). The reaction order of biosorption is dependent upon the characteristics of the heavy metals as well as the nature of the sorption sites available on the biosorbent. As an example, from Figure 11, the maximum uranium biosorption capacity for aerobic granular biomass was estimated to be  $218 \text{ mg g}^{-1}$  dry biomass, and in comparison Sar *et al* reported a maximum uranium uptake of  $541 \text{ mg g}^{-1}$  in *Pseudomonas* dry biomass. Concentration dependence of uranium uptake membrane transport of an ion usually follows the classic Michaelis–Menten enzymatic kinetics model. The half-saturation constant,  $K_m$ , and maximum uptake,  $U_{\text{max}}$ , were derived from these data. The half-saturation constant  $K_m$  and maximum uptake rate  $U_{\text{max}}$  were computed to be  $0.51 \pm 0.07 \text{ mM}$  and  $0.099 \pm 0.005 \text{ mmol} \cdot \text{m}^{-22} \cdot \text{min}^{-21}$ , respectively (see also fitted curve in Figure 2a). The Michaelis–Menten equation was applied to determine binding sites (Fortin 2004).

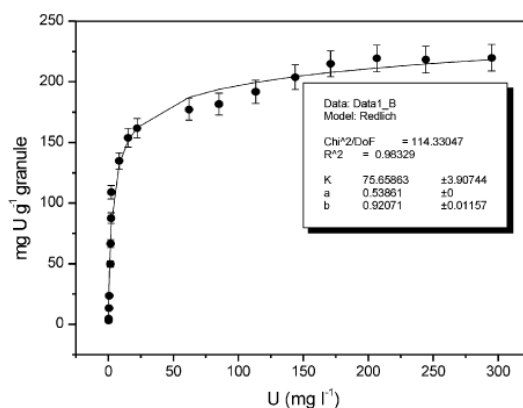


**Figure 11. Biosorption of uranium from solutions of different initial uranium concentrations. Specific uptake of uranium ( $\text{mg U g}^{-1}$  dry biomass) was plotted as a function of uranium remaining in the solution after 24h incubation time. (Source: Nancharaiah)**

**Table 6. Parameters used in Modeling Tracers and U(VI) Adsorption/Desorption for ICE I (Source: John M.Zachara)**

Pore water velocity, $v$	10.36	cm/h	measured
Total porosity, $\theta$	0.30		measured
Dispersion coefficient, $D$	55.2	cm <sup>2</sup> /h	PFBA and Br effluent
Mobile porosity, $\theta_m$	0.24		PFBA and Br effluent
Immobile porosity, $\theta_{im}$	0.06		PFBA and Br effluent
Mass transfer coefficient, $\omega$	$1.82 \times 10^{-2}$	h <sup>-1</sup>	PFBA effluent
	$1.48 \times 10^{-1}$	h <sup>-1</sup>	Br effluent
Sediment bulk density, $\rho_b$	1.91	kg/L	independent estimate
<2 mm size mass fraction	24.7%		independent estimate
<2 mm size bulk density, $\rho_b^f$	0.47	kg/L	independent estimate
Labile U(VI) in <2mm size fraction	454.2	ug/kg	independent estimate
U distribution coefficient, $K_d$	15.5	mL/g	from U desorption
Logarithm mean of rate constant, $\mu$	-6.62	log(h <sup>-1</sup> )	from U desorption
Deviation of log rate constant, $\sigma$	2.69	log(h <sup>-1</sup> )	from U desorption

The model well described the ICE-1 effluent U(VI) in all phases (Figure 17) with the same set of the parameters. In that model, the <2mm size fraction was assumed to be the

### ***Nutrient Uptake, Metabolism and Growth Modeling***

The bacterial production (BP), ug of C /L/Day, can be easily estimated by the leucine incorporated method, or by using the following equation:  $BP = N(e^{\mu_c} - 1) \times V \times F$  where  $N$  is the bacterial count (cells ml<sup>-1</sup>),  $\mu_c$  is mean bacterial growth rate in the control samples,  $V$  is the bacterial cell volume of 0.146  $\mu\text{m}^3$  and  $F$  is the C:V ratio of 120 fg C  $\mu\text{m}^{-3}$  according to Nagata & Watanabe 1990 (as cited in Ichinotsuka 2010). The Ichinotsuka group supported the work by Billen et al. (1990) and Pace & Cole (1994) (as cited in Ichinotsuka 2010) where bacterial cell density is suggested to increase with the increase in bacterial production, implying that bacterial biomass at steady state is a direct function of substrate supply. Thus, bacterial populations can be easily increased with additions of substrates to the soil such as phosphorus, carbon, and nitrogen. Bacteria multiply through binary fusion such that their growth phase follows an exponential curve since every cell will split in two (Tortora). Thus, (initial cell #)\*2<sup>(# of generations)</sup>= (# cells) such that (# of generations)= [log(# cells)-log(initial cell#)]/log(2) so that the growth rate (u) per unit of time is:  $u = [\text{LN}(\# \text{ cells}) - \text{LN}(\text{initial cell } \#)] / (\text{time elapsed between readings})$ .

### ***Uranium Toxicity Modeling***

Using the specific growth rates estimated from the leucine incorporation and bacterial abundance experiments, we can study the sensitivity of the groundwater microbes from the Hanford 300 Area to uranium species. Uranium inhibition of growth was modeled using the following generalized Monod expression demonstrated in Levenspiel Equation:

$$\text{Equation 1. } \frac{u_i}{u_0} = \left( 1 - \frac{[\text{UO}_2^{2+}]}{[\text{UO}_2^{2+}]_{\text{crit}}} \right)^n$$

Where  $u_i$  is the first order growth rate in the presence of  $\text{UO}_2^{2+}$ ,  $u_0$  is the growth rate in  $\text{UO}_2^{2+}$  free medium, and  $[\text{UO}_2^{2+}]$  is the concentration in uM in the medium. The  $[\text{UO}_2^{2+}]_{\text{crit}}$  value, calculated empirically, corresponds to the theoretical minimum  $[\text{UO}_2^{2+}]$  that completely inhibits growth. The exponent,  $n$ , is referred to as the toxic power. The quotient on the left side of the equation is referred to as the relative inhibition, which when plotted against the  $\text{UO}_2^{2+}$

concentrations generates toxicity curves (VanEngelen 2010). As  $n$  approaches zero, the inhibition curve becomes more sharply concave downward and the amount of U required to kill or stun 50% of the total population approaches the  $[UO_2+2]_{crit}$  value. As  $n$  approaches 1, the inhibition curve becomes more linear, and the LD50 approaches half of the  $[UO_2+2]_{crit}$  value. For  $n > 1$  the corresponding inhibition curve becomes concave upward as the LD50 approaches zero.

### ***Uranium Speciation Modeling***

Uranium toxicity and detoxification mechanisms in bacteria depend on concentration and chemical forms of U(VI) that are present (Sani 2006). Uranium speciation in Hanford synthetic ground water was determined using MINTEQA2 version 4.03. The partial pressure of atmospheric CO<sub>2</sub> was incorporated into the model and was assumed to stay constant with a pCO<sub>2</sub> of 10<sup>-3.5</sup>. PIPES buffer was not included in the modeling since no published thermodynamic data for this buffer was found.

### **3.7 Measuring Bacterial Biomass Production and Growth Rates from Leucine Incorporation in Natural Aquatic Environments**

Kirchman (2001) describes how the rate of biomass production is a fundamental property of all organisms in nature; it can be used as a general index of microbial activity and specifically to calculate growth rates. The biomass production can be used to estimate use of dissolved organic material (DOM) if coupled with an estimate of growth efficiency. In short:

#### **Equation 2.**

$$Dissolved\_organic\_material = \frac{bacterial\_biomass\_production}{growth\_efficiency} = \frac{L^{-1}ug\_of\_C * h^{-1}}{fraction} = \frac{B * u}{fraction}$$

Assuming no mortality, bacterial biomass increases exponentially (while not necessarily very quickly), see Figure 12.

$$\text{Equation 3.} \quad \text{Bacterial production} = \frac{dB}{dt} = B * u$$

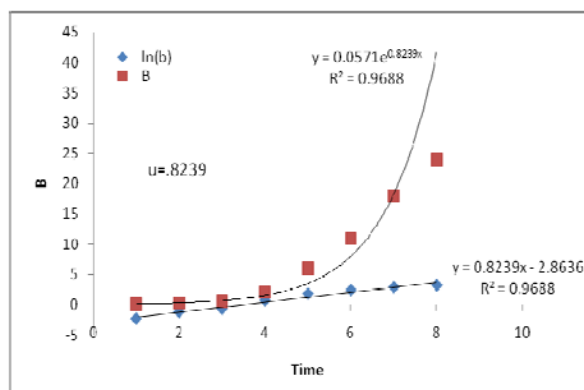
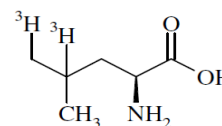


**Figure 12. Example of bacterial biomass exponential growth.**

Although in nature, due to bacterial mortality, the rate is equal to zero, mostly due to grazers and viruses. Experimental work assumes no respiration affecting the rate and no mortality effects; this measures gross production allowed by short incubation time, less than a few hours, compared to the timescale of bacterial growth and mortality (a day or longer). Kirchman et al. (1985) was the first to propose the method of leucine incorporation to estimate bacterial production (Liu 2007). The method is rapid, easy, and specific for heterotrophic bacteria.

### **Leucine Incorporation Principle**

Leu incorporation measures protein synthesis in pure cultures of bacteria because leucine is a constant proportion of all protein, 7.3% according to Kirchman et al., 1985 (as cited in Kirchman 2001). Thus, rates of protein synthesis can be estimated from the rate at which this amino acid appears in the protein fraction (Figure 13); nearly all leucine is incorporated directly into protein. The rates of total biomass production can be estimated in turn if the amount of protein per cell or per cellular mass is known. Cell size and thus protein per cell can vary greatly, but protein is a relatively constant fraction of bacterial biomass (60% of dry weight; according to Simons and Azam, 1989 (as cited in Kirchman 2001)).



M.W. 131  
C<sub>6</sub>H<sub>13</sub>NO<sub>2</sub>

**Figure 13. Leucine amino acid.**

Leucine rates in protein are estimated from the appearance of radioactivity, added as <sup>3</sup>H-Leucine (20nM), in the protein fraction. This amount is much higher than in situ (<1nM), thus, the natural extracellular leucine can be ignored in all calculations, and due to negative feedback the bacteria will up take the exogenous <sup>3</sup>H-Leucine and repress leucine biosynthesis, or non radioactive leucine normally used for protein synthesis. However, some unknown amount of biosynthesis still occurs, thus we will end up making a small dilution of incorporation of radioactive leucine, called isotope dilution (ID).

### **Equation 4.**

$$\text{bacterial\_biomass\_production} = \frac{\text{Leu\_incorp\_moles}}{\text{L*hour}} * \text{Leu\_mw} * \frac{1}{\text{Leu/protein}} * \frac{\text{Cell\_C}}{\text{Protein}} * \text{Isotope\_dilution}$$

**Equation 5.**

$$bacterial\_biomass\_production = \frac{g\_of\_C}{L*hour} = \frac{Leu\_incorp\_moles}{L*hour} * \frac{131.2g}{mol} * \frac{1}{0.073} * \frac{0.86Cell\_C}{Protein} * 1$$

According to Simon and Azam, 1989 (as cited in Kirchman 2001), cellular C per protein is 0.86 and the average isotope dilution is about 2, but a more conservative approach assumes it to be 1. Leucine= HO<sub>2</sub>CCH(NH<sub>2</sub>)CH<sub>2</sub>CH(CH<sub>3</sub>)<sub>2</sub> =131.2g/mol.

**Equation 6.**

$$bacterial\_biomass\_production = \frac{Kg\_of\_C}{L*hour} = \frac{Leu\_incorp\_moles}{L*hour} * \frac{1.5Kg\_of\_C}{mol}$$

**Growth rate from Leucine**

Bacterial production =  $\frac{dB}{dt} = B*u$  and gross production measured by leucine incorporation is then:

**Equation 7.**

$$Specific\_growth\_rate = u = \frac{BP}{B} = \frac{Biomass\_production}{bacterial\_abundance} = \frac{\frac{Kg\_of\_C}{L*hour}}{\left(\frac{cells}{L}\right) * \left(\frac{10*10^{-15}kg\_of\_C}{cells}\right)} = \frac{1}{hour}$$

Note: bacterial biomass is estimated by multiplying by a carbon per cell conversion factor of 10 fg C \* cell<sup>-1</sup> (Fukuda et al. 1998).

Growth rates have units of time<sup>-1</sup> while generation time (g) has units of time:

$$\text{Equation 8.} \quad g = \frac{\ln(2)}{u} = \frac{0.693}{u}$$

Doublings per day is calculated as 1/g. The growth rate calculated from biomass production would reflect an average for the entire bacterial assemblage, including the very slow and the very fast growing cells.

The rate of leucine incorporation as nmol L<sup>-1</sup> h<sup>-1</sup> is:

**Equation 9.**

$$Leu\_incorp = \frac{\{(dpm\_on\_sample) - (dpm\_in\_killed\_control)\}}{incubation\_time * (2.22 * 10^6 dpm / uCi)} * Leu\_specific\_activity\_as\_nmol / uCi$$

The factor 2.22\*10<sup>6</sup> dpm/uCi converts the radioactivity (dpms) found on the sample to uCi, the unit for the leucine specific activity, provided by manufacturer.

### 3.8 Protocol: Measuring <sup>3</sup>H-Leucine Incorporation by the Microcentrifuge Method (Kirchman)

#### *Equipment and reagents*

- Tritiated leucine ([2,3,4-<sup>3</sup>H]leucine) as a stock solution with specific activity >60 nmol/Ci (1 mCi ml<sup>-1</sup>) (NEN, Amersham).
- 2 ml microcentrifuge tubes (polycarbonate material, other should be avoided)
- Pipettes that dispense volumes ranging from microliters to milliliters. Repeating dispensers for the washes and scintillation cocktail
- Trichloroacetic acid (TCA) in concentrated solution (100% w/v) and as a wash solution (5%)
- Ethanol, 80%
- Aspitator, and vortexer
- Scintillation cocktail (7ml). Ultra-Gold (Packard Instruments)
- Microcentrifuge
- 7 ml plastic scintillation vials & scintillation counter
- Appropriate containers for radioactive corrosive liquids and radioactive solids

#### *Treatments*

All in CF-SGW (carbonate-free synthetic groundwater, PIPES buffered, pH 6.7)  
0, 5, 25, 50, 100, 250, 500 uM U and a 0 uM U with no cells.

#### *Assay (Kirchman) variation*

1. Add 0.15ml of a 10X U(VI)-Cl stock of corresponding treatment concentration to 1.35 ml of bacteria resuspended in 1X carbon-free synthetic groundwater and 0.015 ml of <sup>3</sup>H-Leucine.
2. Incubate.
3. Add 75 ul of 100% TCA to kill the bacteria and then cool samples at 4C for an hour.
4. Remove supernatant by aspiration avoiding the pellet after centrifuging (13,000 rpm for 10 min).
5. Add 1.5ml of cold 5% TCA for washing, and repeat step 4.
6. Add 1.5 ml of ice-cold 80% EtOH and repeat step 4.
7. Add 0.2 ml of 1M NaOH to the pellet, vortex and heat slurry at 90C for 1 h in eppy-tube block heater.
8. Add 1.2 ml of scintillation cocktail to the tube and vortex briefly
9. Place microcentrifuge tube in empty 20 ml scintillation vials and radioassay for 30 min.
10. It is usually necessary to allow the sample to sit for as long as two days to maximize the dispersion of the radioactivity into the cocktail.

### 3.9 Cell Count Microscopy

Our microbial samples were preserved and fixed with 1% Glutaraldehyde (2.5ml 10% glutaraldehyde in 22.5 ml of GW) until counted. Utilizing a 0.1 um filter (Millipore HAWP02500) on top of a supporting 0.45 uM filter, samples are vacuumed filtered with a certain volume allowing 1-2 ml to remain on top of the filter. 1 ul/ml of cybergreen dye (EX

488,EM 520 nm) is then added the mix and allowed to sit for 1-5 minutes. Rinse with 1 ml of filtered water and place filter paper on a microscope glass slide. Finally, using 20ul of Citifluor antifade mounting medium (eMS# 17970-25) gently press on the filter paper with a microscope coverslip. Press and wipe clean. Using a fluorescent microscope, count at least 15 fields or 300 bacteria in 7 fields. Always start creating samples from the blank or background sample of sterile water, and then onto those with increasing microbial populations. Taking into account the dilution factor (0.9), the filter effective area ( $2.27\text{E}+8 \text{ um}^2$ ), the filtration volume used (ml), the counting area ( $1.77\text{E}+4$  for the area of the whole field or 7407.121639 for the area covered by one image, see Figure 19), and the average cells per field, then the average cells/ml is:

**Equation 10.** 
$$\frac{\text{cells}}{\text{mL}} = \frac{(\text{Mean\_cells/field}) * (\text{filter\_effective\_area})}{(\text{counting\_Area}) * (\text{Filtration\_volume}) * (\text{dilution\_factors})}$$

TEM could be conducted by washing with DI water, fix with 2.5 % glut, gradual dehydration in ethanol, and infiltration in LR white embedding resin (Sigma, St. Louis, MO). Samples would be sectioned to a thickness of 70 nm on a microtome. Sections are then mounted on a 200 mesh copper grids coated with formvar-support film and sputtered with carbon. Uranium precipitates were identified by TEM in the range of 3 to 5 nm (Sani 2006).

## 4. RESULTS AND DISCUSSION

### 4.1 $^3\text{H}$ -Leucine Uptake Kinetics

The results depicted in Figure 14, conducted by Andrew E. Plymale, details the kinetics of the  $^3\text{H}$ -Leucine incorporated method by the microbes collected from the groundwater in the 300 Area in Hanford. The percent uptake of  $^3\text{H}$ -Leucine was found to have a linear relationship behavior directly proportional to the incubation time over the 18 hours time lapse tested. From these results, we established that 20 hours of incubation time should be used for further results since we want to ensure at least 1% uptake to correctly show decrements as a result of U toxicity, and account for cell density variability. We have also confirmed, by testing the control treatment or natural groundwater with 0.25X, 0.5X, and 1X the natural cell density, that the activity or percent uptake of  $^3\text{H}$ -Leucine is also directly proportional to the cell density of these microbes.

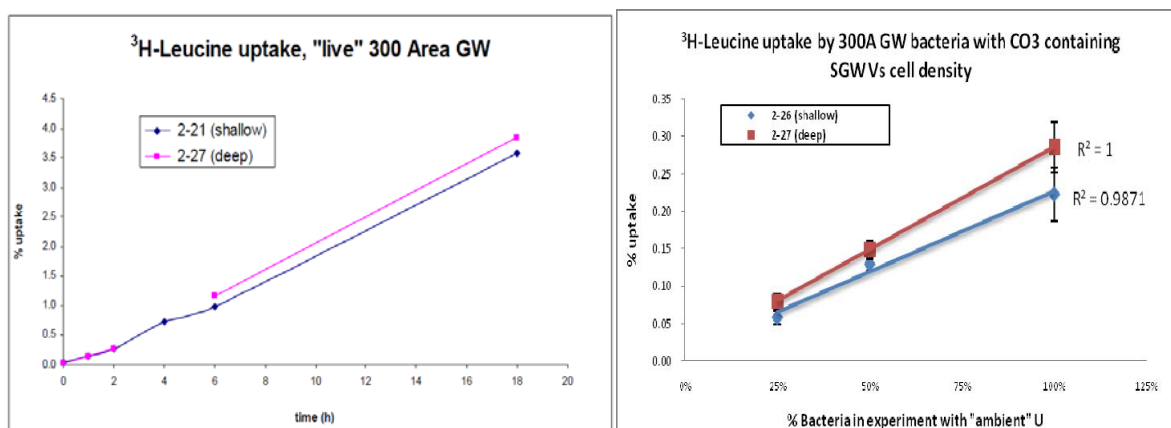


**Figure 14. [Left] Groundwater collected 5-10-10. Well 2-21 (water table depth- 31 ft bgs) was bailed, while well 2-27 (deep) was pumped. Leucine was at 500 nM (2.5 uCi/sample). Incubation was at RT (static). [Right] Groundwater from wells 2-26 & 2-27 with 500 nM  $^3\text{H}$  leucine in 10 hr incubation time with 0.25X, 0.5X, and 1X the natural cell density. Provided by Andrew E. Plymale.**

Since the microbes are present in the 300 Area groundwater that contains uranium and carbonate, the first  $^3\text{H}$ -Leucine toxicity assay was performed by adding more uranium to the natural groundwater to determine the highest uranium concentration tolerable before it became toxic to the microbes. Because of the uranyl phosphate and uranyl bicarbonate complexes, only high concentrations of U are expected to be toxic (Sani 2006). As anticipated, our results, shown in Figure 15, support these observations. Of all the different uranium concentrations added to the natural groundwater uranium levels,  $\approx 12 \mu\text{M}$  to  $250 \mu\text{M}$  of added uranium showed no significant signs of cell activity inhibition since the percentage of leucine uptake varied very little when compared to the control. If the current trend follows, we expect that approximately  $500 \mu\text{M}$  of added uranium concentration would be toxic to the microbes. These results suggest that seasonal fluctuating groundwater levels and the mobile uranium plume in the 300 Area that varies the concentration of soluble uranium in the groundwater will not, to a great extent, affect the microbial population unless U speciation and its bioavailability is changed.

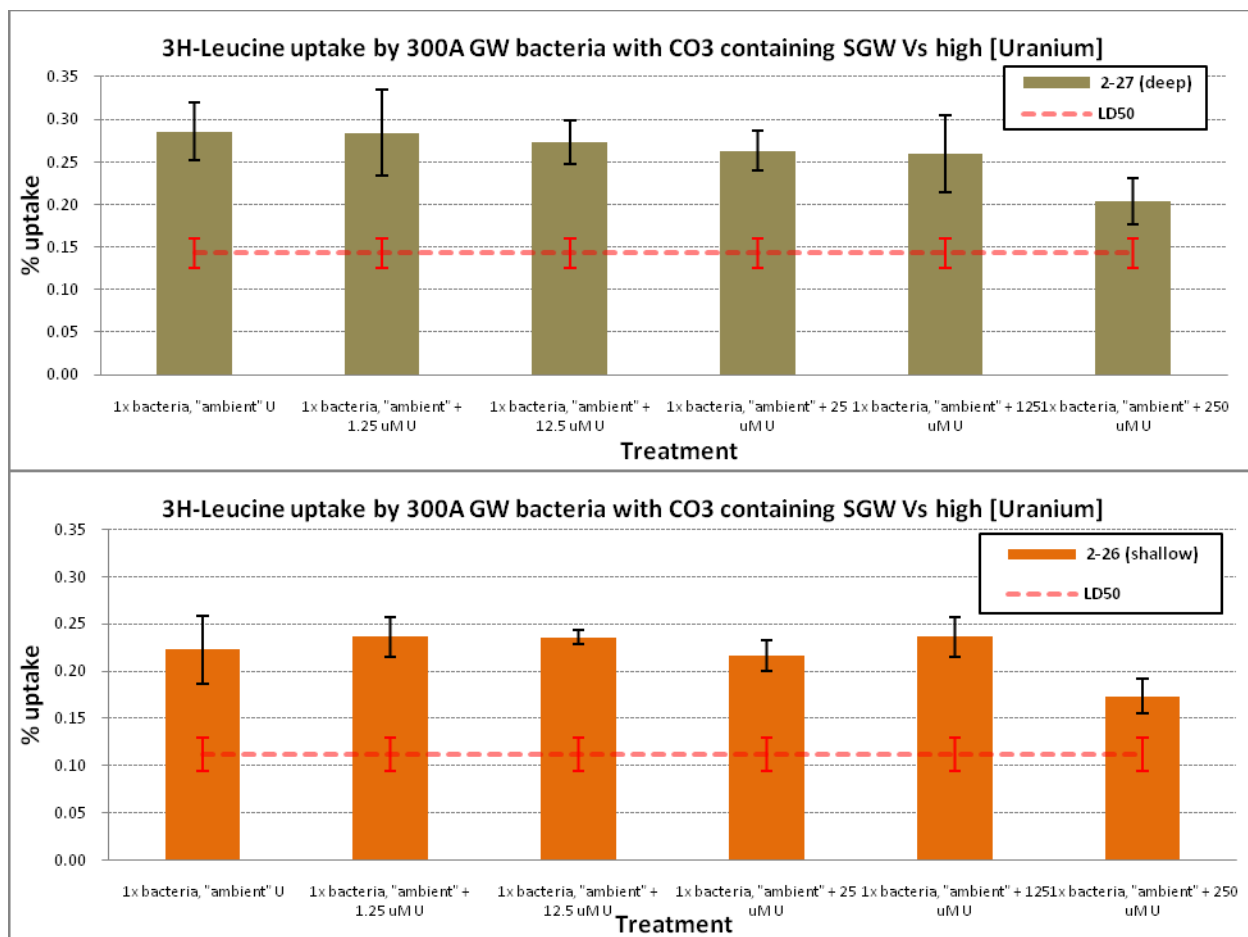


**Figure 15. Groundwater was collected 5-29-10. Both well 2-26 (water table depth) and well 2-27 (deep) were pumped. Leucine was at 500 nM (2.5 uCi/sample). Samples were incubated with 3H-Leu for 10 h (RT, static).**

**All treatments contained 2.5 mM added NaHCO<sub>3</sub> and were diluted 9/10 in the NaHCO<sub>3</sub>/U(VI) stock.**

**Provided by Andrew E. Plymale. (n=3)**

The results from the 3H-Leucine uptake toxicity assay for the 300 Area groundwater in CO<sub>3</sub>-free Pipes-Synthetic Groundwater are very different when compared to the same experiment conducted in natural groundwater. All the different concentrations of uranium tested, from 5 uM to 500 uM, produced no significant leucine uptake indicative of microbial activity. Furthermore, since all results were well below the lethal dose, 50% (LD<sub>50</sub>), the uranium concentration required to kill half the members of the tested population after the specified test duration that we use as an indication of toxicity, we concluded that all concentrations tested are toxic to the microbes as shown in Figure 16. In contrast to the experiment with natural CO<sub>3</sub> containing groundwater from Figure 15, with up to 250 uM of added uranium, where the cells thrived as indicated by their activity via the high percentage of leucine uptake compared to that of the control, the important role of the CO<sub>3</sub> complexes for protecting and promoting cell survival and activity become significant. No CO<sub>3</sub> containing treatment reached the LD<sub>50</sub>. Also, there was no significant difference between the microbes on either the shallow or deep well from this experiment. To ensure that the results were not a reflection of pH changes, we checked the pH of our treatments with a pH meter and found no pH difference from the original 6.7 pH between the 5-20 uM U

treatments (data not shown). pH from the 100 uM U and above treatments became more acidic than the original. The  $\approx 1$  mM of PIPES used was most likely insufficient for the high concentrations,  $>100$  uM, of U added.

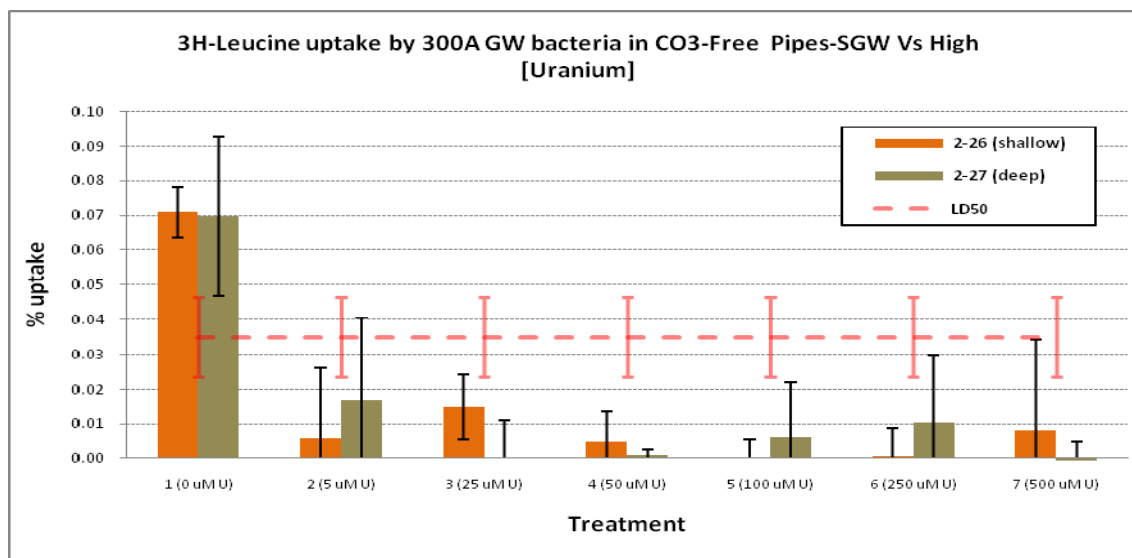


**Figure 16. 3H-Leucine incorporated uranium toxicity study: 300A GW bacteria from the deep & shallow wells in CO<sub>3</sub>-Free PIPES SGW Vs high uranium concentrations (pH 6.7). All treatments killed more than 50% of the microbial population, thus all treatments were above the lethal dose of uranium under these conditions. (n=3)**

Further testing of the same wells with the same conditions with lower uranium concentration, 0-5 uM, in the 3H-Leucine uptake toxicity assay for the 300 Area groundwater microbes in CO<sub>3</sub>-free Hepes-Synthetic Groundwater revealed the LD<sub>50</sub> to be 0.3 uM of U. For both the deep and shallow well microbes results showed less than 50% activity than the control (Figure 17). This shows how remarkable the uranium carbonate complex is by protecting the cell from uranium's toxic effects most likely due to the reduced U bioavailability as previously discussed. The presence of carbonate complexes made the LD<sub>50</sub> concentration an estimated 1,597 times larger, from 0.313uM U in CO<sub>3</sub>-free Hepes- synthetic groundwater to 500uM U in natural CO<sub>3</sub>-containing groundwater.

It is also apparent that the H3-Leucine uptake in the 2-27 deep well is approximately 29 times greater than the 2-26 shallow well. This significant difference cannot be concluded to be differences in the microbial population activities or susceptibility due to their location in reference to the groundwater and the uranium plume. We believe this is due to the different concentration of cells recovered from the process of filtering and re-suspending the microbes from the 300 Area groundwater to the U-free synthetic groundwater;  $\approx 100\%$  recovery for the 2-27 deep well or  $1.91\text{E}+5$  cells/ml vs.  $\approx 10\%$  for the 2-26 shallow well or  $7.59\text{E}+3$  cells/ml (Figure 18). The re-suspensions cell numbers proportionately match the 3H-Leucine uptake results,  $\approx 25\text{x} \pm 20$  times more cells versus  $\approx 29\text{x} \pm 4$  more Leucine uptake in the deep-well samples (2-27), in comparison to the shallow (2-26). These conclusions are based on the fluorescence microscopy

counts of the microbes like those seen in Figure 19. It is also very apparent from the microscope images that the cells in the deep well (2-27) tend to be more morphologically larger and elongated like rods when compared to the smaller cocci shaped shallow well (2-26).

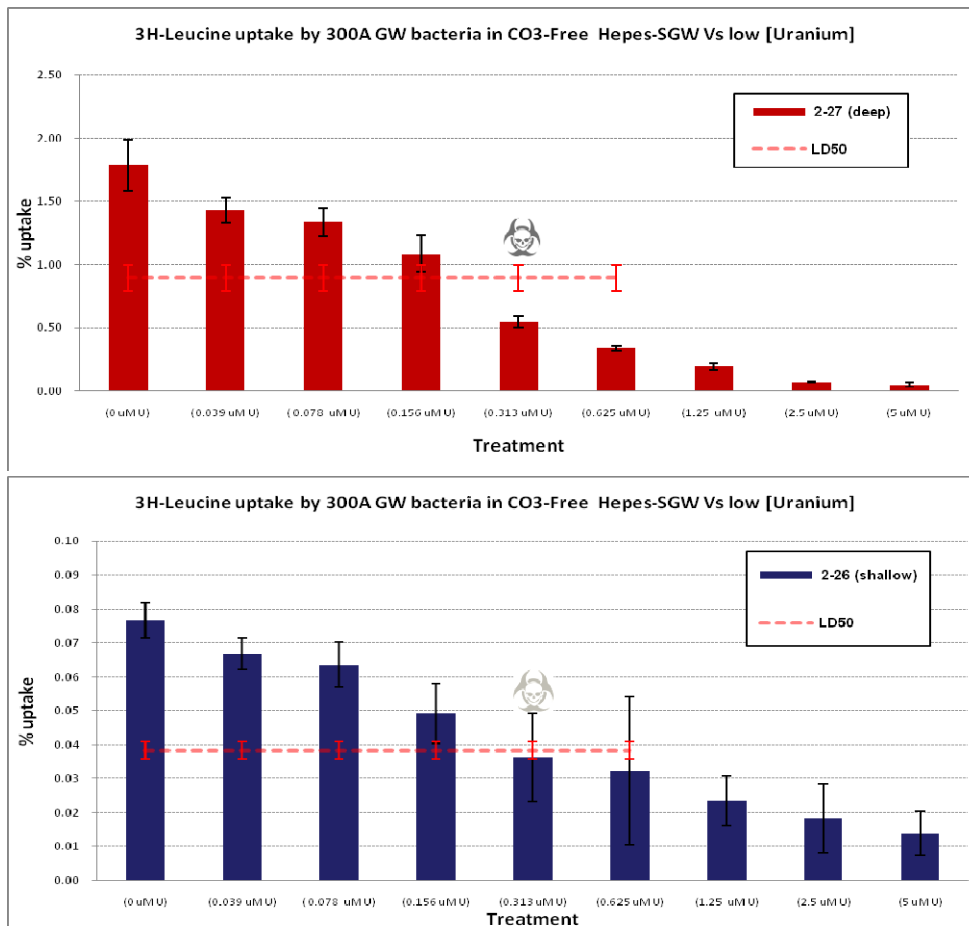


**Figure 17. 3H-Leucine incorporated uranium toxicity study: 300A GW bacteria resuspended in CO<sub>3</sub>-free HEPES SGW pH 7.7 (2 mM HEPES, ~ 0.25 mM HCO<sub>3</sub><sup>-</sup> from atmospheric CO<sub>2</sub>) vs Low uranium concentrations from: A) the deep wells, B) shallow wells. Lethal dose occurs at the 0.3 uM of Uranium. (n=3)**

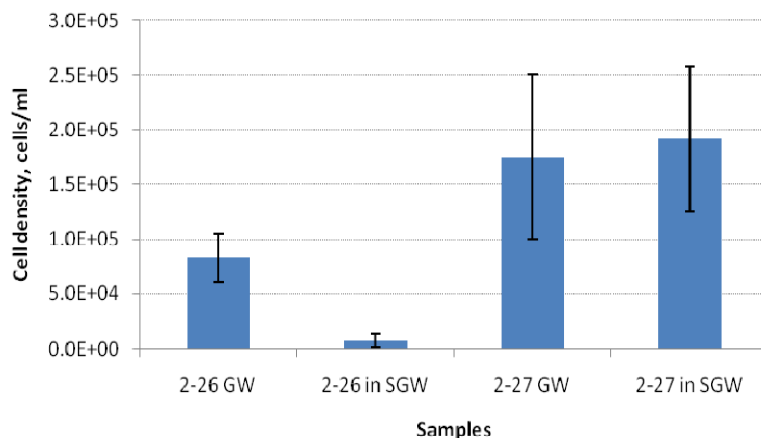


**Figure 18. Cell density (cells/ml) of microbes fresh from the groundwater vs. cell density (cells/ml) of microbes filtered and re-suspended in the synthetic groundwater used for experiments from both the deep (2-27) and shallow (2-26) wells.**

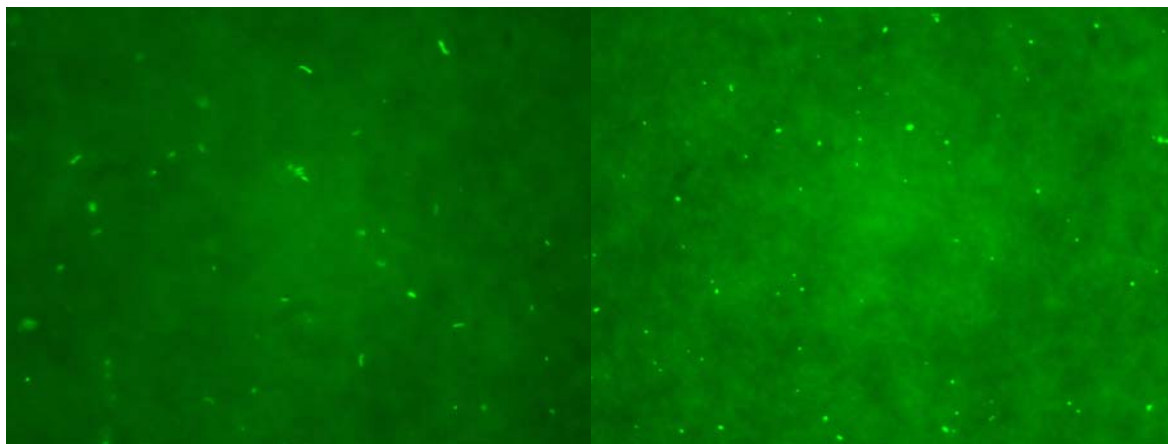


**Figure 19. Fluorescent microscopy camera field view of the Cybergreen Fluorescence staining on the 2-27 (deep) & 2-26 (shallow) 300 Area microbes (left and right respectively). (Source: Dr. Xueju Lin)**

When testing the shallowest well 3-23 and repeating the 2-26 shallow well with low uranium concentrations, 0-5 uM, in the 3H-Leucine uptake toxicity assay for the 300 Area groundwater microbes in CO<sub>3</sub>-free Pipes-Synthetic Groundwater, the data is reproducible for 2-26 having 0.3 uM U to be the LD<sub>50</sub>. However, for the shallowest 3-23 well, the toxic effects of uranium are much more prominent, its LD<sub>50</sub> was 0.03uM U. All concentrations higher than the LD<sub>50</sub> for both the deep or shallow well microbes showed less than 50% activity than the control (Figure 20). Since the lowest natural uranium groundwater level measured between all 3 wells was 0.079 uM U, these results confirm how the uranium carbonate complex is protecting the cell from toxic effects most likely due to reduced bioavailability as discussed previously.

The previously mentioned H3-Leucine uptake in the 3-23 shallow well is approximately 40 times greater than the 2-26 shallow well. This significant difference is most likely attributed to the differences in the microbial population activities and increased susceptibility to uranium effects in reference to their location in the groundwater and the uranium plume. Since the 3-23 well

bacteria abundance is only 1.3 time greater than the 2-26 well, we do not attribute any difference in their activities due to any change in the concentration of cells recovered from the process of filtering and re-suspending the microbes from the 300 Area groundwater to the U-free synthetic groundwater:  $\approx 1.26\text{E}+4$  cells/ml for the 3-23 well vs.  $\approx 9.8\text{E}+3$  cells/ml for the 2-26 shallow well (Figure 18 and Figure 21). These conclusions are based on the fluorescence microscopy counts of the microbes like those seen in Figure 19. There were no apparent differences between the microbes of these two wells under the microscope images, other than the presence of the occasional algae cells in the 2-26 well.

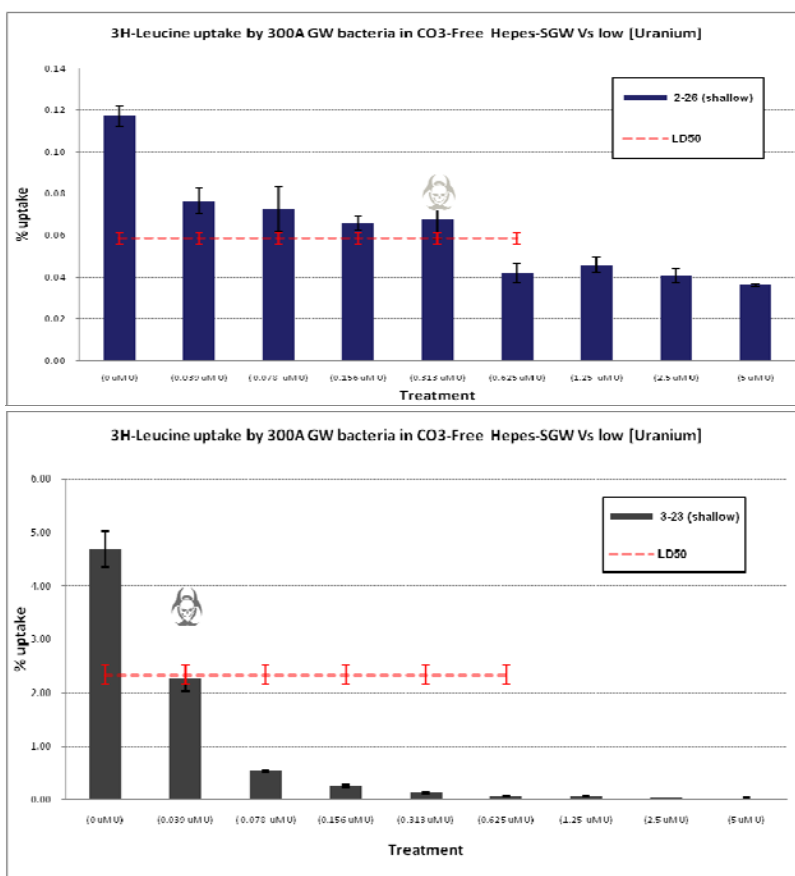


**Figure 20. 3H-Leucine incorporated uranium toxicity study: 300A GW bacteria resuspended in CO<sub>3</sub>-free HEPES SGW pH 7.7 (2 mM HEPES,  $\sim 0.25$  mM HCO<sub>3</sub><sup>-</sup> from atmospheric CO<sub>2</sub>) vs Low uranium concentrations from: Top) 2-26 shallow well. Bottom) 3-23 shallow well. (n=3)**

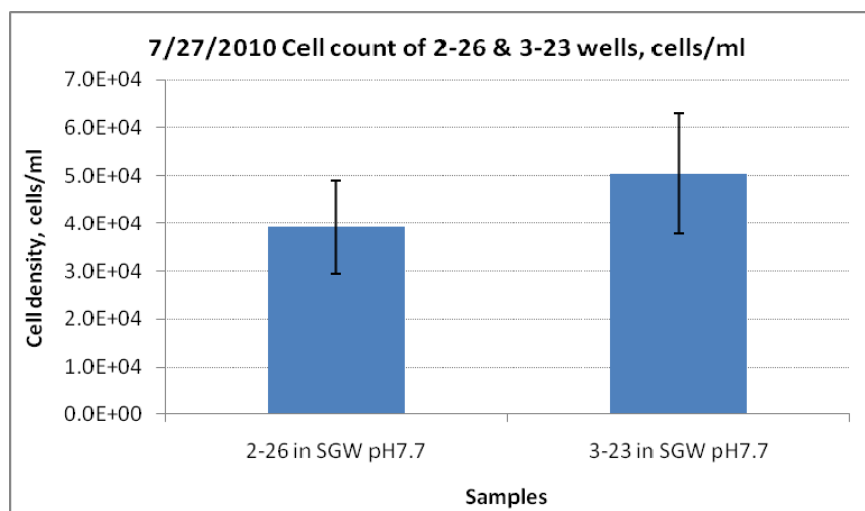


**Figure 21.** Cell density (cells/ml) of microbes filtered and re-suspended in the synthetic groundwater used for experiments from both the (3-23) and (2-26) shallow wells.

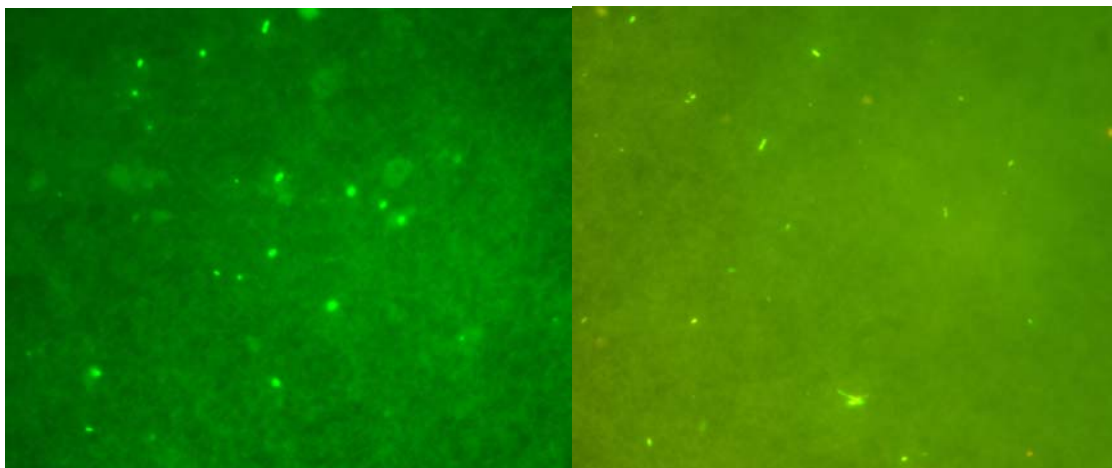


**Figure 22.** Fluorescent microscopy camera field view of the Cybergreen Fluorescence staining on the 300 Area microbes of the 3-23 & 2-26 wells (left and right respectively). (Source: Dr. Xueju Lin)

The measured natural uranium background over time is not constant. These fluctuations are expected to mimic the rise and fall of the water table level of the Columbia River. KPA analysis revealed that the 3-23 well, which was the most responsive to the toxic effect to uranium, is the sample that is least exposed to uranium. Its natural background level was well below the EPA standard, 0.079uM U, (Figure 23). The 2-26 shallow well is  $\approx 33$  feet deep followed by the 2-27 deep well which is  $\approx 58$  feet deep. The shallowest well, 3-23, was measured to 31.3 feet deep. These KPA results are in close agreement with the average calculated in the IFRC October 2009 Uranium Desorption Experiment results.

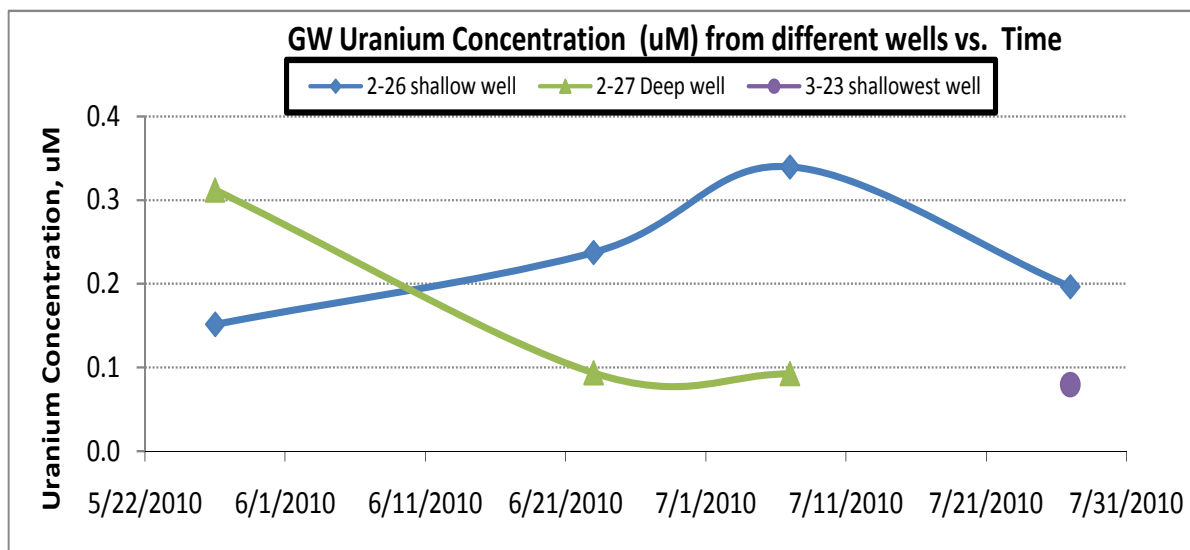


**Figure 23. Measured natural uranium background concentrations over time for the 300 Area groundwater via KPA analysis.**

The toxic power (n) model was fitted to our data. The results shown in Figure 24, are in good agreement with our observations. Results from 7-7-10 model confirm U (VI) sharp toxicity via the rapid exponential decline of the % inhibition as the concentration increases to 5 uM. The results from 7-27-10 model underestimates U(VI) toxicity for 2-26 but is very accurate for the 3-23 well. The higher the power, the n value, the more toxic uranium becomes to the sample group. Thus, the 3-23 well with a n value equal to 60 is the most toxic among the 2-26 and 2-27 well that have an n value equal to 13.5 and 15.4, respectively.

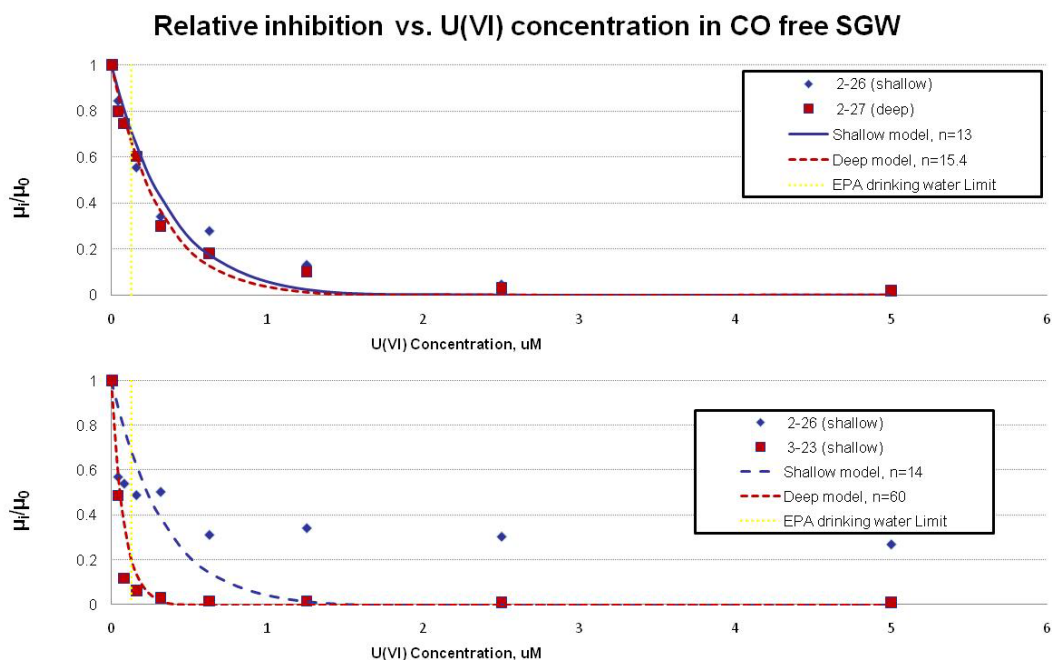


**Figure 24. Relative inhibition vs. U(VI) concentration in CO free SGW, (top) 7/7/10 experiments, (bottom) 7/27/10 experiments. Toxic power (n) model.**

MINTEQA2 modeling of the speciation of uranium under the different treatments tested for the leucine incorporated method provides some insightful results as shown in (Figure 25). Based on the results, the species that changed in concentration the most with added uranium was  $(\text{UO}_2)_3(\text{OH})^{5+}$ . It is more likely that toxicity in our experiments, in an open system where  $\text{CO}_2$  is allowed to equilibrate, is ruled by this species. The fact that it is a trimetric form of uranium, and that it's the most positive species, gives it the most potential to interact and damage the negatively charged cell. For example, there are 113.3  $(\text{UO}_2)_3(\text{OH})^{5+}$  molecules per cell vs. ~209 million molecules per cell, in the 0.03 vs. 5 uM U with ambient  $\text{CO}_2$ , that is 1.8 millions time greater. Similarly, ~96 million molecules  $(\text{UO}_2)(\text{CO}_3)_2^{-2}$  per cell Vs. ~11.8 Billion molecules per cell, 0.03 Vs. 5uM U with ambient  $\text{CO}_2$ ; that is only 123 times greater. The change in concentration of these positive species perfectly mimics the 3H leucine uptake results as shown in Figure 25. In contrast, MINTEQA2 modeling of the 0.3 uM U with increasing carbonate concentrations shown in Figure 26, prove our hypothesis and confirms the results from literature that the carbonate complexes uranium reducing the positive species and making uranium less bioavailable to the negatively charged cells.

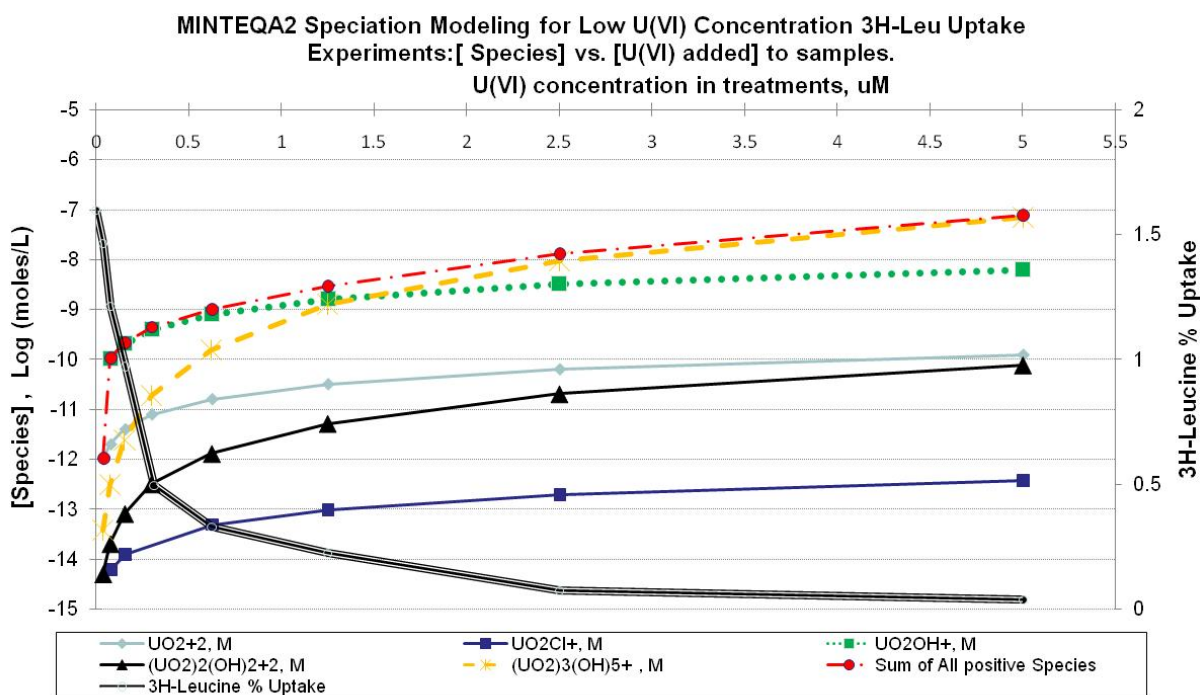


**Figure 25. U toxicity to bacteria as 3H-Leu % uptake from 300A groundwater re-suspended in  $\text{CO}_3$ -free SGW, pH 7.7 (2 mM HEPES, ~0.25 mM  $\text{HCO}_3^-$  from atmospheric  $\text{CO}_2$ ), and concentration of uranium positive species vs uranium concentration.**

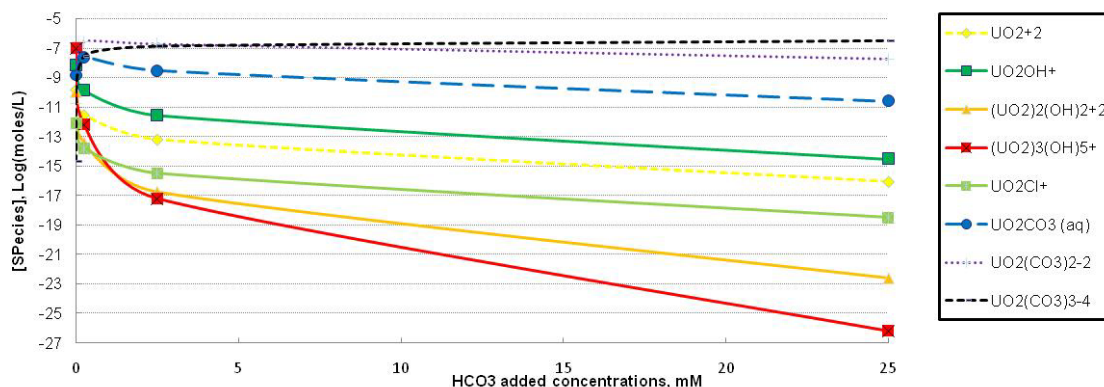


**Figure 26. MINTEQA2 uranium speciation modeling: [Species] vs. increasing [HCO<sub>3</sub>] added to SGW with 0.31  $\mu$ M (UVI) with atmospheric equilibration ( $\sim 0.2$  mM HCO<sub>3</sub>).**

Andrew Plymale lead by A. Konopka determined that phosphorus by itself is not a significant contributor to the growth of the 300 Area soil and groundwater microbes (Figure 27). They tested the Hanford sediment ( $\sim 13$ - $34.9''$  deep), and the Ringold sediments ( $\sim 59$ - $60''$  deep), which had greater cell numbers and 3H-Leucine activity uptake compared to the Hanford sediment, when studying Tritiated leucine (3H-leucine) uptake;  $4 \times 10^6$  compared to  $2 \times 10^6$  cells/ml, and  $1.5 \times 10^{-19}$  compared to  $4.6 \times 10^{-20}$  moles 3H-Leucine uptake cell<sup>-1</sup> h<sup>-1</sup> respectively. However, the result was the same for both soils tested. Additions of C (0.046 mM acetate, 0.031 mM lactate, 0.015 mM glucose), N (0.033 mM NH<sub>4</sub>Cl), and P (0.0032 mM Na<sub>2</sub>HPO<sub>4</sub>) to sediment/groundwater slurry (0.3 g sediment, wet weight, per ml groundwater) in all possible combinations revealed that carbon is the most likely nutrient limiting factor for the growth of this microbial populations that is under oligotrophic conditions (Figure 27).

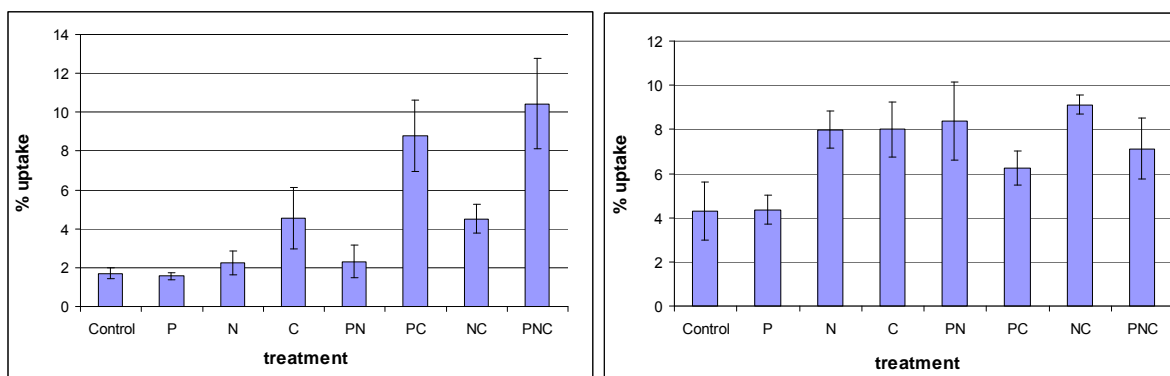


**Figure 27. 3H-Leucine uptake by bacteria desorbed from Hanford (left) and Ringold (right) sediments amended with C, N, and P. Produced and provided by Andrew E. Plymale.**

## 5. CONCLUSION

---

Ultimately, the impact of heavy metals and other environmental contaminants on humans and other organisms depends on their concentration levels, toxicity, and bioavailability (Brown 1999). We have shown this to be true, in the uranium contaminated soil and groundwater of the Hanford 300 Area, near the Columbia River in southeastern Washington state, by studying the different toxic effects of varying uranium concentrations and how they fluctuate depending on factors such as pH and carbonate concentrations, which determine its bioavailability to the microbes. The microbes are resilient enough to withstand high concentration levels of uranium if chelating agents like carbonate are present to protect it. The 3H-Leucine incorporation method that provides biomass production (gC per liter per day) information was implemented to quantify microbial biomass activity and uranium toxicity with success. Results show that carbonate is a dominant variable that determines the uranium speciation and toxicity to the microbial community. Toxicity is mitigated by the presence of tightly binding  $\text{UO}_2^{+2}$  ligands, including bicarbonate species, and dissolved organic carbon (DOC), both of which can form stable  $\text{UO}_2^{+2}$  complexes (VanEngelen 2010). This work will help develop more accurate understanding and adaptable models to predict the fate and transport of uranium in the subsurface. Stimulating the growth of the bacteria has potential remedial value for uranium contaminated aquifers. The research presented here is part of a large effort to advance the understanding of the biogeochemistry processes and plausible remediation strategies concerning the uranium plume in the Hanford 300 Area.

## 6. FUTURE WORK

---

Uranium is not the only contaminant in the 200/300 Area of Hanford that requires attention. Cr(VI),  $^{137}\text{Cs}$ , and  $^{99}\text{Tc}$  could be studied and evaluated the same way as we have planned for uranium for comparison and to look into any beneficial properties between the microbe and actinide interactions to understand the natural processes in the field. Because *Arthobacter* is primarily a vadose zone organism at Hanford, the study will focus on the soil and groundwater at this vadose zone. It would also be of interest to study any interactions with the native minerals, such as boltwoodite, found in some areas at Hanford.

## 7. REFERENCES

---

- Brooks, Scott, et al. "Inhibition of Bacterial U(VI) Reduction by Calcium." Environ Sci Technol 37 (2003): 1850-1858.
- Brown, Gordon E., Jr., Andrea L. Foster, and John D. Ostergren. "Mineral surfaces and bioavailability of heavy metals: A molecular-scale perspective." Proc Natl Acad Sci 96 (1999): 3388-3395.
- Crocker, F.H., J.K. Fredrickson, D. C. White, and D. B. Ringelberg. "Phylogenetic and physiological diversity of Arthrobacter strains isolated from unconsolidated subsurface sediments." Microbiology 146 (2000): 1295-1310.
- Demoling, Fredrik, Daniela Figueroa, and Erland Baath. "Comparison of factors limiting bacterial growth in different soils." Soil Biology & Biochemistry 39 (2007): 2485-2495.
- Fortin, Claude, et al. "Uranium complexation and uptake by a green alga in relation to chemical speciation: the importance of the free Uranyl Ion." Environmental Toxicology and chemistry 23.4 (2004): 974-981.
- Fowle, David A., Fein, and B.Jeremy. "Experimental Measurements of the reversibility of metal-bacteria adsorption reactions." Chemical Geology 168 (2000): 27-36.
- Gorman-Lewis, Dre, et al. "Adsorption of aqueous uranyl complexes onto bacillus subtilis cells." Environmental Science and technology 39 (2005): 4906-4912.
- Ichinotsuka, Daisuke, Et al,. "Effects of nutrient supplies on the growth rates of planktonic bacteria in Uchiumi Bay, Japan." Aquatic Biology Vol.9 (2010): 123-130.
- Fredrickson, James K., John M. Zachara, David L. Balkwill, David Kennedy, Shu-mei W. Li, et al. "Geomicrobiology of High-Level Nuclear Waste-Contaminated Vadose Sediments at the Hanford Site, Washington State." Appl.Environ.Microbiol. 70 (2004): 4230-4241.
- Kelly, S.D., et al. "Ca-UO<sub>2</sub>-CO<sub>3</sub> Complexation – Implications for Bioremediation of U(VI)." Physica Scripta T115 (2005): 915-917.
- Kirchman, David. "Measuring Bacterial Biomass Production and Growth Rates from Leucine Incorporation in Natural Aquatic Environments." Methods in Microbiology 30 (2001).
- Konopka, Allan, et al. "Microbial Ecology in Subsurface Sediments from Hanford 300A Area." SFA, PNNL Microecol. Poster (Oct 2009).
- Lin, Xueju, David Kennedy, Jim Fredrickson, and Allan Konopka. Distribution of microbial biomass and the potential for anaerobic respiration in Hanford Site subsurface sediments. Poster. Richland, Wa.: ASM, 2009.
- Liu, Chongxuan, et al. "Influence of Calcium on Microbial Reduction of Solid Phase Uranium(VI)." Biotechnology Bioengineering 97.6 (2007): 1415-1422.

- McKinley, James P., Et al. "Geochemical controls on Contaminant Uranium in Vadose Hanford formation sediments at the 200 and 300 area, Hanford Site, Washington." Vadose zone Journal Vol.6.4 (2007): 1004-1017.
- McKinley, James P., et al. "The deep vadose zone as a source of uranium to the near-shore aquifer at the Hanford Site, Washington." Abstract-A689. 2010.
- Miettinen, Ilkka T., Terttu Vartiainen, and Pertti J. Martikainen. "Phosphorus and Bacterial growth in drinking water." Applied and environmental microbiology 63.8 (1997): 3242-3245.
- Morris, Donald P., and William M. Lewis, Jr. "Nutrient limitation of bacterioplankton growth in Lake Dillon, Colorado." Limnol Oceanogr 37.6 (1992): 1179-1192.
- Nakajima, Akira, Et al. "Ion effect on the uptake of uranium by chlorella regularis." Agric Biol Chem 43.3 (1979): 625-629.
- Nancharaiyah, Y.V., Et al. "Aerobic granular biomass a novel biomaterial for efficient uranium removal." Current Science 91.4 (2006): 503-509.
- Rozsak, D.B., Colwell, R. R. "Metabolic Activity of Bacterial Cells Enumerated by Direct Viable Count." Applied and environmental microbiology 53.12 (1987): 2889-2983.
- Sani, Rajesh K., et al. "Toxic Effects of Uranium On Desulfovibrio Desulfuricans G20." Environmental Toxicology and Chemistry 25.5 (2006): 1231-1238.
- Selenska-Pobell, Sonja, et al. "Selective accumulation of heavy metals by three indigenous Bacillus strains, B. Cereus, B. megaterium and B sphaericus from drain water of uranium waste pike." FEMS Microbiology Ecology (1999): 59-67.
- Suzuki, Yoshinori, Kazuya Tanaka, Naofumi Kozai, Toshihiko ohnuki. "Effects of Citrate, NTA, and EDTA on the reduction of U(VI)." Geomicrobiology Journal 27 (2010): 245-250.
- Tortora, Funke, Case. Microbiology an introduction. sixth edition. Menlo Park: Benjamin/Cummings Publishing Company, 1998.
- VanEngelen, Michael R., et al. "UO<sub>2</sub>+2 Speciation Determines Uranium Toxicity and Bioaccumulation in an Environmental Pseudomonas Sp. Isolate." Environmental Toxicology and Chemistry 29.4 (2010): 763-769.
- Wellman, Dawn M., et al. "Effects of pH, temperature, and aqueous organic material on the dissolution kinetics of meta-autunite minerals, (Na, Ca)<sub>2</sub>-1[(UO<sub>2</sub>)(PO<sub>4</sub>)]<sub>2</sub>\* 3H<sub>2</sub>O." American Mineralogist, Vol 91, (2006): 143-158.
- Zachara, John M., The IFRC Reseach Team. "Hanford IFRC Quarterly Final Report 10-13-09." Pasific Northwest National Laboratory (2009).